

Water Resources Research®

RESEARCH ARTICLE

10.1029/2023WR036297

Key Points:

- A novel framework combining interpretable machine learning and cluster techniques was proposed to investigate flash drought mechanism
- Four distinct types of driving mechanisms of flash drought onset in eastern China were discovered
- Nearly 70% of flash drought events involve multiple mechanisms, emphasizing the time-varying feature of drought drivers

Supporting Information:

Supporting Information may be found in the online version of this article.

Correspondence to:

J. Li and Z. Wang,
junli_lucky@pku.edu.cn;
wangzh1@scut.edu.cn

Citation:

Feng, J., Li, J., Xu, C.-Y., Wang, Z., Zhang, Z., Wu, X., et al. (2024). Viewing soil moisture flash drought onset mechanism and their changes through XAI lens: A case study in eastern China. *Water Resources Research*, 60, e2023WR036297. <https://doi.org/10.1029/2023WR036297>

Received 23 SEP 2023

Accepted 31 MAY 2024

Author Contributions:

Conceptualization: Jiajin Feng, Jun Li, Chong-Yu Xu, Zhaoli Wang, Shijie Jiang

Data curation: Jiajin Feng

Formal analysis: Jiajin Feng

Funding acquisition: Jun Li,

Hongfu Tong

Investigation: Jiajin Feng

Methodology: Jiajin Feng, Jun Li, Chong-Yu Xu, Shijie Jiang

Project administration: Jun Li

Resources: Jun Li, Hongfu Tong

Software: Jiajin Feng, Jun Li






Supervision: Jun Li, Zhaoli Wang,

Shijie Jiang

© 2024. The Authors.

This is an open access article under the terms of the [Creative Commons Attribution-NonCommercial-NoDerivs License](https://creativecommons.org/licenses/by/4.0/), which permits use and distribution in any medium, provided the original work is properly cited, the use is non-commercial and no modifications or adaptations are made.

Viewing Soil Moisture Flash Drought Onset Mechanism and Their Changes Through XAI Lens: A Case Study in Eastern China

Jiajin Feng¹, Jun Li^{1,2} , Chong-Yu Xu³ , Zhaoli Wang^{1,4} , Zhenxing Zhang⁵, Xushu Wu¹ , Chengguang Lai^{1,4}, Zhaoyang Zeng¹, Hongfu Tong⁶, and Shijie Jiang^{7,8} 

¹State Key Lab of Subtropical Building Science, School of Civil Engineering and Transportation, South China University of Technology, Guangzhou, China, ²Sino-French Institute for Earth System Science, College of Urban and Environmental Sciences, Peking University, Beijing, China, ³Department of Geosciences, University of Oslo, Oslo, Norway, ⁴Pazhou Lab, Guangzhou, China, ⁵Illinois State Water Survey, Prairie Research Institute, University of Illinois, Champaign, IL, USA, ⁶Qingyuan Hydrology Sub-Bureau of Guangdong Province, Qingyuan, China, ⁷Max Planck Institute for Biogeochemistry, Jena, Germany, ⁸ELLIS Unit Jena, Jena, Germany

Abstract Soil moisture flash droughts often pose significant challenges to humans and ecosystems, with wide-ranging socioeconomic consequences. However, the underlying mechanisms of flash droughts and their changes remain unquantified. Taking China as a case study, we present a novel framework that combines machine learning with interpretable and cluster techniques to investigate flash drought mechanisms from 1980 to 2018. We first quantified the temporal contribution of drivers and further identified different mechanisms during drought onsets. We subsequently investigated the temporal changes in different mechanisms and classified drought event types. We identified four driving mechanism types triggering drought: Concurrent precipitation, Antecedent-concurrent precipitation, Antecedent temperature-concurrent precipitation, and Antecedent transpiration-concurrent precipitation. The total effects from vegetation transpiration contributed to around 50% of the impacts for mechanisms involving antecedent transpiration and concurrent precipitation, highlighting the non-neglectable role of vegetation water consumption in drought occurrences. Remarkably, about 60% of flash drought onsets exhibited close association with the antecedent anomalies, which contribute approximately 50% of overall effects, emphasizing the importance of the cumulative effects of drivers. Moreover, driving mechanisms associated with temperature and transpiration increased significantly over time, implying an elevated influence of these factors on droughts. Our classification of drought events reveals that nearly 70% of events were driven by at least two mechanisms, underscoring a complex time-varying pattern of driving factors during drought events. The proposed holistic framework not only sheds insight into the multifaceted mechanisms driving flash droughts within China but also extends its potential applicability to broader geographical contexts.

1. Introduction

Drought is a recurring natural disaster that poses significant risks to water resources, agriculture, and socio-economics (Kuwayama et al., 2019; J. Li et al., 2023; Stanke et al., 2013; van Dijk et al., 2013; Veijalainen et al., 2019; Yuan et al., 2023). Mounting evidence suggests a potential increase in drought's frequency, duration, and severity and a shift in inherent characteristics across the globe in the 21st century (Cook et al., 2020; T. Wang et al., 2021). Drought is traditionally regarded as a slow and long-lasting phenomenon (J. Li, Wang, Wu, Chen, et al., 2020; Wilhite et al., 2007). However, in the context of global warming, soil moisture can evolve rapidly during short-term periods (i.e., days and weeks) and are termed “flash droughts” (Otkin et al., 2018; Svoboda et al., 2002). Soil moisture flash droughts have attracted a great deal of attention from the scientific community and stakeholders (Lisonbee et al., 2021) due to their devastating impact on agricultural production (Boyer et al., 2013), fire potential (L. Wang & Yuan, 2018), inland navigation (Grigg, 2014), ecosystem health (Xi & Yuan, 2022), and economic development (Basara et al., 2019). Therefore, understanding the dynamics and mechanism of soil moisture flash droughts is crucial for developing effective mitigation and adaptation strategies in the face of changing climate conditions.

Recently, there has been a surge in investigations into the mechanism of flash droughts. Mo and Lettenmaier (2015) introduced a classification of flash droughts into two types, that is, heat wave and precipitation deficit

Validation: Jiajin Feng

Writing – original draft: Jiajin Feng,
Jun Li, Chong-Yu Xu, Zhaoli Wang,
Shijie Jiang

Writing – review & editing: Jiajin Feng,
Jun Li, Chong-Yu Xu, Zhaoli Wang,
Zhenxing Zhang, Xushu Wu,
Chengguang Lai, Zhaoyang Zeng,
Shijie Jiang

types, and suggested that heat wave droughts were associated with elevated evapotranspiration (ET) due to high temperature (Tem), while precipitation deficit droughts were related to precipitation (Prec) and ET reduction. However, such a definition overlooked the rapidly evolving nature of flash drought. Subsequently, L. Wang and Yuan (2018) highlighted the swift intensification of droughts and investigated the potential drought drivers by analyzing anomalies in relevant drivers (i.e., Tem, Prec, and ET) during both the antecedent and onset phases of droughts. Mukherjee and Mishra (2022) employed similar methods to investigate the driving factors of flash drought, uncovering a lagged impact of Prec changes on the evolution of such events. However, the investigation with meteorological anomalies potentially neglects the quantitative relationships between the drivers and droughts (Q. Zhu & Wang, 2021).

Several methods, including multiple linear regression (Noguera et al., 2022; L. Wang et al., 2016), logistic regression (Ford & Labosier, 2017), and water balance equation (Koster et al., 2019), have been proposed to quantify the impact of flash drought drivers. In these studies, flash droughts have been categorized based on concurrent meteorological anomalies, such as those driven by simultaneous high-Tem or concurrent Prec deficits (L. Wang & Yuan, 2018). Some studies that consider antecedent meteorological conditions have not systematically quantified the individual contributions of different variables to specific events (Ford & Labosier, 2017). Nevertheless, the cumulative effect of drivers (i.e., how both antecedent and concurrent climatic conditions contribute to the flash droughts onset), as well as the time-varying interplay between drivers and the whole events (i.e., the number of distinct driver types identified in connection with a flash drought), remain unclear. Therefore, the development of a novel framework to quantitatively explore the cumulative effect of drivers and their temporal pattern within an event becomes imperative, facilitating a more profound understanding of the flash drought mechanism.

Moreover, the relationship between vegetation activities and droughts, especially flash drought, has been frequently investigated (Ahmad et al., 2022; L. Chen et al., 2021; Guo et al., 2023; Otkin et al., 2016; Piao et al., 2020; Xi & Yuan, 2022; M. Zhang et al., 2022). Recent studies have underscored that flash drought occurrences could be indeed associated with vegetation activities (S. Li & Sawada, 2022; W. Li et al., 2022). For example, an increase in global greening can result in elevated transpiration, exacerbating the depletion of soil moisture (L. Chen et al., 2021; M. Zhang et al., 2022). Guo et al. (2023) found that the enhanced transpiration anomalies have contributed to the intensification of soil moisture drought in China. Under climate change, the contribution of vegetation transpiration to the reduction of soil moisture is projected to amplify (M. Li et al., 2022). Overall, these studies suggest the important role of vegetation water consumption in the occurrence and development of flash drought (L. Chen et al., 2021; M. Zhang et al., 2022). The consideration of transpiration thus becomes imperative when dissecting the specific attributions of drought events (Song et al., 2020).

In recent years, the utilization of machine learning (ML) within the realm of earth and hydrology science has witnessed a notable surge, driven by its capability to process massive data sets and untangle complicated relations between drivers and response factors (Karpatne et al., 2019; Reichstein et al., 2019). However, the complex network structure and huge parameter space in certain ML algorithms, such as deep learning, have posed challenges in comprehending the underlying mechanics (Jiang et al., 2022; Mamalakis et al., 2022; Roscher et al., 2020). In this case, eXplainable Artificial Intelligence (XAI) recently has become a topic of intense research, driven by the pressing need for humans to unravel the complex mechanisms and rationales (Linardatos et al., 2020; Samek & Müller, 2019). It has demonstrated its ability to obtain novel knowledge in several research areas related to earth and hydrological science, including climate patterns (Toms et al., 2020), flood forecasting (Ding et al., 2020), ecosystem effects (M. Li et al., 2022; W. Li et al., 2022), flooding mechanism (Jiang et al., 2022), and long-lasting drought mechanism investigation (Dikshit & Pradhan, 2021a, 2021b). These studies illustrate that XAI holds the potential to uncover the cumulative effects and time-varying patterns of drivers on dependent variables. Hence, it is imperative to employ this cutting-edge technique to gain insights into the implicit linear or non-linear interplay between the potential drivers and soil moisture flash droughts, thereby advancing our understanding of the mechanisms behind flash droughts.

This study introduces a novel framework aimed at investigating the mechanism of soil moisture flash droughts and the spatial-temporal changes in their mechanisms, employing XAI. More precisely, we first trained long short-term memory (LSTM) to predict soil moisture using key potential drivers (i.e., Prec, Tem, and Tran). Subsequently, the trained LSTM models were seamlessly integrated with an interpretation algorithm (expected gradients (EG)) to create XAI models. These XAI models were then employed to assess the temporal

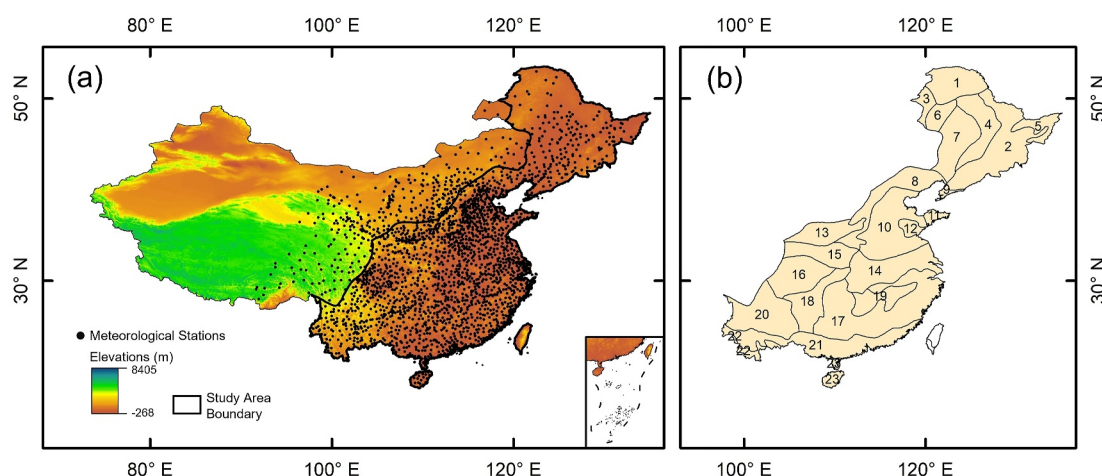


Figure 1. (a) Geographical locations of the study area and meteorological stations. (b) The 23 sub-areas employed in this study. The numbers in (b) represent the ID for each sub-area, corresponding to the first column in Table S1 in Supporting Information S1.

contributions (the values of EG sequences) of individual inputs to soil moisture flash droughts. Building upon this, we incorporate cluster analysis to categorize diverse types of flash drought onset and quantitatively discern the potential impacts of associated factors. We finally analyzed the spatial and temporal change for different types of events associated with different mechanisms. Overall, this study contributes to the understanding of mechanisms behind flash drought and extends the state-of-the-art XAI application within the realm of hydrology. Our framework possesses the potential for generalization and application to the analysis of various other extreme events, such as floods and heat waves, across different spatial scales.

2. Data and Methods

2.1. Data and Study Area

In this study, eastern China was taken as a case study (Figure 1a). This region was deliberately selected due to its recurrent instances of flash droughts (L. Wang et al., 2016; L. Zhang et al., 2021), with projections indicating an escalating risk of such events in the future (Yuan et al., 2019). This contextual backdrop offered a highly suitable backdrop for our analytical pursuits. For training XAI models, the study area was further divided into 23 sub-areas according to their aridity type and geographic attributes (Figure 1b), which were obtained from the Resources and Environmental Sciences Data Center, Chinese Academy of Sciences (<http://www.resdc.cn>). The detailed information on the sub-areas can be seen in Table S1 in Supporting Information S1.

In this study, the daily root-zone soil moisture and Tran from 1980 to 2018 was acquired from Global Land Evaporation Amsterdam Model (GLEAM) with a spatial resolution of $0.25^\circ \times 0.25^\circ$ (Martens et al., 2017; Miralles et al., 2011) and was resampled to a 0.5° resolution with bilinear interpolation. The Tran and soil moisture data have been extensively employed in drought analysis, consistently demonstrating their reliability in drought monitoring (J. Li, Wang, Wu, Xu, et al., 2020; J. Li et al., 2022; Poppe Terán et al., 2023; Uribe & Dukes, 2021). Daily meteorological data sets from 1980 to 2018, including precipitation, mean air temperature, relative humidity (RH), and wind speed (WS), were collected from 2,278 observational stations managed by the China Meteorological Administration (<http://data.cma.cn/>) across China (Figure 1a). The data sets were interpolated to $0.5^\circ \times 0.5^\circ$ spatial resolution by using the inverse distance weighting method to match the spatial scale of the soil moisture data set. All the aforementioned data sets were converted to pentad (5-day) mean time series to match the timescale of flash drought identification.

2.2. Overall XAI Framework for Flash Drought Driving Factors Attribution

The general framework of XAI-based flash drought driving factors quantitative attribution encompasses the following main steps, as illustrated in Figure 2.

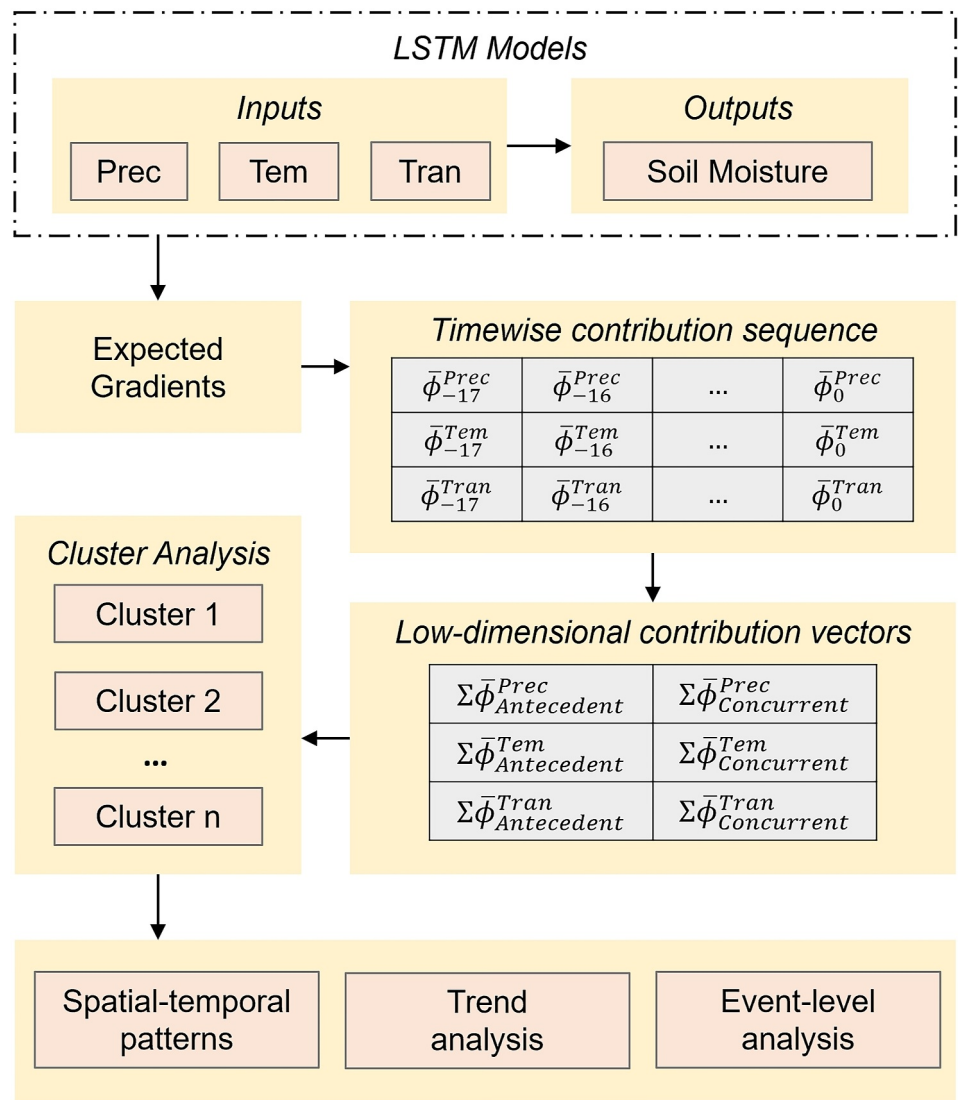


Figure 2. Flow chart of the flash drought mechanism identification based on eXplainable Artificial Intelligence.

Step I establishes a nonlinear predictive relationship between the potential drivers and soil moisture with LSTM models. Notably, precipitation deficit and elevated temperature have been recurrently linked to flash drought occurrences (Mo & Lettenmaier, 2015; L. Wang & Yuan, 2018). Moreover, recent studies underscore the potential role of anomalous vegetation water consumption, typified by heightened transpiration, in flash drought occurrence (L. Chen et al., 2021; M. Zhang et al., 2022). Other variables, such as evapotranspiration, evaporation, and vapor-pressure deficit (VPD), have a certain impact on soil moisture flash droughts (P. Li et al., 2024; Mahto & Mishra, 2023). Evapotranspiration consists of transpiration from plants and evaporation from soil, open water surfaces, and canopy-intercepted water (Wei et al., 2017). However, transpiration constitutes a major proportion (approximately 60%) in evapotranspiration (Lian et al., 2018; Niu et al., 2019). Additionally, air temperature has a substantial effect on evaporation (Kalma et al., 2008), which makes up a fraction of evapotranspiration. Since temperature and transpiration have been considered as potential flash drought drivers, we exclude evapotranspiration and evaporation as potential drivers. In addition, VPD is a comprehensive index that incorporates RH and temperature (Mahto & Mishra, 2023), and can show a high correlation with temperature. Therefore, VPD is also excluded as a potential driver, and we established LSTM models for all sub-areas with Prec, Tem, and Tran as input variables, and soil moisture as output variables.

Step II couples the trained LSTM models with an XAI technique, termed EG (Erion et al., 2021), to quantify the temporal contribution of input variables in predicting soil moisture. With the EG method, we can acquire the quantitative impact of potential drivers (Prec, Tem, and Tran) on soil moisture depletion at different time steps. We here identified soil moisture flash drought events following the method proposed by Yuan et al. (2019) based on its widespread utilization and good performance for identifying soil moisture flash drought in recent years (Xi & Yuan, 2023; Yuan et al., 2023; M. Zhang et al., 2022; Y. Zhang et al., 2021). First, to represent soil moisture changes, soil moisture data was converted into percentiles throughout the same pentads for each year during 1980–2018. Second, when the soil moisture percentile decreases from above the 40th percentile to below the 20th percentile, with a decline rate of no less than 5% percentile for each pentad, an onset of a flash drought event is determined. Finally, a flash drought event terminates when soil moisture percentile rises up to the 20th percentile, or the length of the flash drought event reaches 12 pentads (Christian et al., 2019; J. Li, Wang, Wu, Chen, et al., 2020). We note that the maximum duration of a flash drought event was set at 12 pentads (60 days) to distinguish the long-lasting drought. If a detected flash drought event lasts longer than 12 pentads, we will focus on the initial 12 pentads to analyze the drivers of flash drought onset. We then applied the EG method to quantify the contribution of input variables for each time step within flash droughts.

Step III analyzes the contribution of input variables with EG calculated in Step II. We aggregated each EG sequence into a low-dimensional contribution vector according to their time period. Subsequently, we employed cluster analysis to categorize these contribution vectors into distinct groupings to identify different mechanisms of flash drought onsets. We further investigated the spatio-temporal changes in each category. Moreover, we also classified different types of flash drought according to the categories they contained to gain insight into the mechanisms of flash droughts across the study area.

2.3. Long Short-Term Memory

Long short-term memory (Hochreiter & Schmidhuber, 1997) is an improved form of recurrent neural network (RNN), which is designed to overcome the problems of gradient vanishing of traditional RNN and capable of learning long-term dependencies (Fu et al., 2016; Kratzert et al., 2018). The input of each LSTM cell consists of x_t which is the input vector of the current time step, h_{t-1} which is the output of the LSTM cell at the previous time step, and C_{t-1} which is the cell state of the LSTM cell at the previous time step. The output of each LSTM cell consists of h_t which is the output of the LSTM cell at the current time step and C_t which is the cell state of the LSTM cell at the current time step. Each LSTM cell contains three gates: forget gate f_t , input gate i_t , and output gate o_t . The forget gate decides how much of the previous cell state needs to be forgotten. The input gate decides the new information that would be added to the current cell state C_t . The output gate determines the retention degree of the cell state to h_t in the current time step. \tilde{C}_t is the new candidate values calculated from x_t and h_{t-1} . The relations mentioned above can be described as follows:

$$f_t = \sigma(W_f \cdot [h_{t-1}, x_t] + b_f) \quad (1)$$

$$i_t = \sigma(W_i \cdot [h_{t-1}, x_t] + b_i) \quad (2)$$

$$\tilde{C}_t = \tanh(W_C \cdot [h_{t-1}, x_t] + b_C) \quad (3)$$

$$C_t = f_t * C_{t-1} + i_t * \tilde{C}_t \quad (4)$$

$$o_t = \sigma(W_o \cdot [h_{t-1}, x_t] + b_o) \quad (5)$$

$$h_t = o_t * \tanh(C_t) \quad (6)$$

where σ denotes the sigmoid function, $*$ denotes the element-wise multiplication, \tanh is hyperbolic tangent function, W_f , W_i , W_C , and W_o denote the matrices of weights from the forget gate, input gate, cell state, and output gate respectively, b_f , b_i , b_C , and b_o denote the bias parameters associated with forget gate, input gate, cell state and output gate respectively.

In this study, the input layer of LSTMs includes Prec, Tem, and Tran of the current pentad and the antecedent 17 pentads (i.e., $[X_{-17}^{\text{Prec}}, X_{-16}^{\text{Prec}}, X_{-15}^{\text{Prec}}, \dots, X_{-1}^{\text{Prec}}, X_0^{\text{Prec}}; X_{-17}^{\text{Tem}}, X_{-16}^{\text{Tem}}, X_{-15}^{\text{Tem}}, \dots, X_{-1}^{\text{Tem}}, X_0^{\text{Tem}}; X_{-17}^{\text{Tran}}, X_{-16}^{\text{Tran}}, X_{-15}^{\text{Tran}}, \dots, X_{-1}^{\text{Tran}}, X_0^{\text{Tran}}]$);

in which the subscript “0” represents the current pentad; the subscript “ $-n$ ” stands for n pentads before the current pentad; the ellipsis represents the time steps ranging from the -14 to the -2 pentads). The output layer produces the soil moisture of the current pentad (i.e., $[y_0]$). The selection of 18 time steps has been thoughtfully considered to encompass the sub-seasonal-to-seasonal timeframes (spanning weeks to months) relevant to flash drought events (Pendergrass et al., 2020). The choice is also informed by prior studies suggesting that meteorological conditions several months preceding the onset of flash droughts could wield an influence on events (L. G. Chen et al., 2019). To mitigate the inherent stochasticity associated with ML model training, we employed a strategy involving the training of three distinct and independent LSTM models for each individual sub-area. The data set in each sub-region was split into a training set and a validation set in a 7-to-3 proportion. The training and validation sets were established through a random selection process, while we note that the selected time periods were consistent for every grid within a given sub-area, maintaining spatial and temporal independence of training and validation data sets. The Nash-Sutcliffe coefficient of Efficiency (NSE) (Nash & Sutcliffe, 1970), the Kling-Gupta Efficiency (KGE) (Gupta et al., 2009; Kling, 2012), the Normalized Mean Absolute Error (nMAE), the Normalized Root Mean Square Error (nRMSE), and Percent bias (PBIAS) were applied to evaluate the predictive performance of the validation set for each sub-area.

2.4. Interpretation Method and Cluster Analysis

In this study, we employed a ML interpretation method termed EG, which was developed by Erion et al. (2021). EG was improved from another XAI method, namely Integrated Gradients (IG) (Sundararajan et al., 2017). The IG for the i th input feature calculates an integrated gradient that aggregates local gradients over a simplified straight-line path ($\gamma(\alpha) = x' + \alpha(x - x')$, and $\alpha \in [0, 1]$) from the baseline input x' ($\alpha = 0$) to the target input x ($\alpha = 1$), and can be described as:

$$\Phi_i^{IG}(f, x, x') = (x_i - x'_i) \times \int_{\alpha=0}^1 \frac{\partial f(x' + \alpha(x - x'))}{\partial x_i} d\alpha \quad (7)$$

The target input refers to a specific data point for which the model's prediction is required for explanation. The baseline input serves as a reference point for comparing against the target input when calculating feature contributions. At baseline input, the network is assumed to predict nothing (Jiang et al., 2022). $\partial f(x' + \alpha(x - x'))/\partial x_i$ denotes the local gradient of the network f at a point interpolated between the baseline input x' and target input x .

The EG method was developed to overcome the problem of selection of baseline input x' in IG method (Jiang et al., 2022), which is expressed as:

$$\Phi_i^{EG}(f, x, x') = \int_{x'} \left((x_i - x'_i) \times \int_{\alpha=0}^1 \frac{\partial f(x' + \alpha(x - x'))}{\partial x_i} d\alpha \right) p_D(x') dx' \quad (8)$$

The EG method assumes that the baseline input x' follows an underlying distribution from sampling the training data set ($x' \in D$), and p_D stands for its density function. Directly integrating over the distribution of training data set is difficult. Therefore, the two integrals involved in Equation 8 can be regarded as expectations (Erion et al., 2021) and Equation 8 can be reformulated as:

$$\Phi_i^{EG}(f, x) = E_{x' \sim D, \alpha \sim U(0,1)} \left[(x_i - x'_i) \times \frac{\partial f(x' + \alpha(x - x'))}{\partial x'_i} \right] \quad (9)$$

In Equation 9, $U(0,1)$ denotes the uniform distribution between 0 and 1. In the calculation of EG, we first draw sample x' from the training data set and draw α from the uniform distribution $U(0,1)$. Next, we compute the value inside the expectation for each sample, followed by averaging the computed values over all samples (Erion et al., 2021). Overall, $\Phi_i^{EG}(f, x)$ denotes the EG score for the input feature x (which is Prec, Tem or Tran in this case) at the i th time step. A positive or negative value of $\Phi_i^{EG}(f, x)$ indicates that the feature x at the i th time step

increase or decrease the output (which is soil moisture in this case). A larger absolute value indicates a more significant impact.

In this study, we performed the calculation of EG with the Shapley Additive exPlanations (SHAP) package (Lundberg & Lee, 2017). We first identified flash drought pentads (Yuan et al., 2019). Based on data sets from 1980 to 2018, we calculated EG values to quantify the influence of drivers (Prec, Tem, and Tran) on soil moisture anomaly in all identified flash drought pentads. Flash drought events in 1980 were not considered due to the possible unavailability of the drivers at the preceding 17 pentads. Each EG sequence has the same dimensions as the input variables (i.e., $[\phi_{-17}^{\text{Prec}}, \phi_{-16}^{\text{Prec}}, \dots, \phi_0^{\text{Prec}}; \phi_{-17}^{\text{Tem}}, \phi_{-16}^{\text{Tem}}, \dots, \phi_0^{\text{Tem}}; \phi_{-17}^{\text{Tran}}, \phi_{-16}^{\text{Tran}}, \dots, \phi_0^{\text{Tran}}]$). The three sequences for each flash drought pentad were averaged into one sequence (i.e., $[\bar{\phi}_{-17}^{\text{Prec}}, \bar{\phi}_{-16}^{\text{Prec}}, \dots, \bar{\phi}_0^{\text{Prec}}; \bar{\phi}_{-17}^{\text{Tem}}, \bar{\phi}_{-16}^{\text{Tem}}, \dots, \bar{\phi}_0^{\text{Tem}}; \bar{\phi}_{-17}^{\text{Tran}}, \bar{\phi}_{-16}^{\text{Tran}}, \dots, \bar{\phi}_0^{\text{Tran}}]$).

In order to reduce subjectivity and uncertainty in the classification of contribution sequences, we applied cluster analysis to group the contribution sequences into several categories. To avoid the heavy computational burden of multi-dimensional time series clustering while retaining feature importance information, we aggregated each ensemble EG sequence into a low-dimensional contribution vector with only six elements $[\sum \bar{\phi}_A^{\text{Prec}}, \sum \bar{\phi}_C^{\text{Prec}}, \sum \bar{\phi}_A^{\text{Tem}}, \sum \bar{\phi}_C^{\text{Tem}}, \sum \bar{\phi}_A^{\text{Tran}}, \sum \bar{\phi}_C^{\text{Tran}}]$, where $\sum \bar{\phi}_A$ and $\sum \bar{\phi}_C$ represent the sum of contribution of a variable during the antecedent and concurrent periods, respectively. The output of explainable LSTM models can be deconstructed into the sum of individual contributions from features (Lundberg & Lee, 2017). In this study, the concurrent periods are defined as the pentads during a flash drought event, and the antecedent periods are defined as the pentads before the onset of a flash drought event. The LSTM's input layer incorporates potential drivers (Prec, Tem, and Tran) for the current pentad and the preceding 17 pentads. Consequently, the length of an EG sequence for each driver at a certain pentad spans 18 pentads. Given the maximum duration of flash drought events is 12 pentads in this study, some of the 18 pentads in an EG sequence fall within the antecedent period (preceding flash drought onset), while the rest pertain to the concurrent period (during the flash drought event). For example, the low-dimensional contribution vector calculated from the EG sequence of the third pentad during a flash drought event should be $[\sum_{-17}^{-3} \bar{\phi}^{\text{Prec}}, \sum_{-2}^0 \bar{\phi}^{\text{Prec}}, \sum_{-17}^{-3} \bar{\phi}^{\text{Tem}}, \sum_{-2}^0 \bar{\phi}^{\text{Tem}}, \sum_{-17}^{-3} \bar{\phi}^{\text{Tran}}, \sum_{-2}^0 \bar{\phi}^{\text{Tran}}]$. We next applied the K-means method to cluster the aggregated feature contribution vectors into groups with similar patterns to obtain an overall picture from the individual results for drought periods from all sub-areas (Forgy, 1965). We applied the silhouette score (Rousseeuw, 1987) to determine the optimal number of clusters for the K-means algorithm. Silhouette score ranges from -1 to 1 , with a higher value usually indicating a better cluster number choice. After the optimal cluster number is determined, the EG values corresponding to the variables within each cluster will be transformed into normalized contributions, expressed as percentages.

Moreover, the mean frequency, duration, severity, and intensity of flash drought events were calculated for each grid cell to characterize flash droughts across the study area. The mean frequency is defined as the average number of flash drought events per year, and the mean duration is the average number of days for which an event lasts. The mean severity is defined as the mean accumulated soil moisture percentile deficit from the threshold of 40%, and the intensity is the average of the largest soil moisture percentile deficit (J. Li et al., 2021).

2.5. Event-Level Analysis

To enhance our understanding of the mechanism of flash drought events, we categorized each drought event based on the groups of contribution vectors present within each event. Precisely, within a flash drought event, if a single cluster of contribution vectors constitutes more than 75% of the overall count, it assumes a dominant role in shaping the event. In scenarios where the largest group represents less than 75%, we assess the proportional shares of the two or three most significant groups. If their combined proportion exceeds 75%, they will dominate the event. Alternatively, if none of the above conditions are met, the event will be classified as a mixed mechanism. Recognizing that the proposed threshold of 75% was determined subjectively, we also conducted two different thresholds (i.e., 60% and 85%) and obtained similar results.

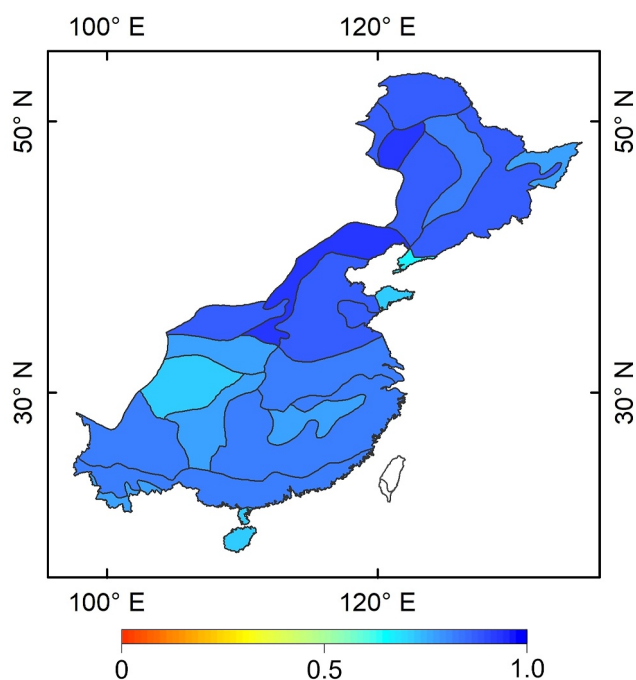


Figure 3. Nash-Sutcliffe coefficient of Efficiency values for the validation sets averaged over the three independent long short-term memory models for each sub-area.

3. Results and Discussion

3.1. Model Predictive Performance and Characteristics of Flash Drought Events

The NSE metric to assess LSTM models is shown in Figure 3. The NSE values ranged from 0.68 to 0.94 across all sub-regions, and their area-weighted value reached 0.84. These results indicate that LSTM models performed accurately for the prediction of soil moisture. In addition, the results of KGE, nMAE, nRMSE, and PBIAS all indicated satisfactory results (Figure S1 in Supporting Information S1). Overall, the LSTM constructed in this study is deemed reliable in establishing predictive relationships and further obtaining meaningful information from the established models (Linardatos et al., 2020; Murdoch et al., 2019).

The average frequency, duration, severity, and intensity are shown in Figure 4. Overall, flash drought events occurred more frequently in the south region than in the north region of east China (Figure 4a), while the duration of flash drought events in the north region was generally longer than that of events in the south region (Figure 4b). A generally higher severity and lower intensity in the north region were detected (Figures 4c and 4d), which is consistent with findings in the previous studies (L. Wang et al., 2016; Yuan et al., 2019).

We conducted further analysis to examine the seasonal patterns of the average frequency, duration, severity, and intensity of flash droughts (Figure S2 in Supporting Information S1). Generally, most events occurred during summer, followed by autumn and spring (Figures S2a–S2c in Supporting Information S1), but few events were detected in winter (Figure S2d in Supporting Information S1). Flash droughts in the northern part of east China were predominantly observed in summer, whereas in the southern part, they occurred not only in summer but also in spring and autumn. In addition, the duration of autumn droughts was longer than that of droughts in spring and summer in southern China (Figures S2e–S2g in Supporting Information S1). Moreover, we found that severity in southern China was higher in summer and autumn than in spring (Figures S2i–S2l in Supporting Information S1), while the intensity did not exhibit significant seasonal patterns (Figures S2m–S2p in Supporting Information S1).

3.2. The Relationship Between Drivers and EG Values

Using the established explainable LSTM models, we calculated the EG contribution sequences of the potential drivers. To distinguish the contributions of drivers during antecedent and concurrent periods, the high dimension of EG sequences was converted into low-dimensional vectors. We then applied the *K*-means clustering algorithm to identify different types of drought mechanisms. The silhouette scores and relevant analysis (Figure S3 in Supporting Information S1) suggest that the optimal cluster number is four.

We here investigated the relationships between the potential drivers and their respective EG values, which represent the temporal impact of these drivers on soil moisture. Notably, antecedent Prec, antecedent Tem, antecedent Tran, and concurrent Prec exhibited non-linear relationships with their associated EG values (Figures 5a, 5b, and 5d). Given that EG values can shed insight into both linear and non-linear effects of drivers on soil moisture, these observed relationships indicate a complex interplay between flash drought drivers and soil moisture (S. Li et al., 2016; Sehler et al., 2019). Specifically, the curves depicted in Figures 5a and 5d reveal that a reduction in EG non-linearly corresponds to a decrease in antecedent or concurrent precipitation. The reduced rate of EG appears to be less than that of precipitation, suggesting that under dry soil, the sensitivity of soil moisture reduction to decreased precipitation could diminish (B. Zhu et al., 2020). Additionally, an increase in percentiles of antecedent temperature is associated with a decline in EG, and the decline rate of EG increases when antecedent Tem is higher (Figure 5b). This implies that under higher antecedent temperature conditions, the sensitivity of soil moisture reduction to increased temperature intensifies. These findings of non-linearity also suggest that exploring flash drought mechanisms solely through the lens of superficial driver anomalies may experience

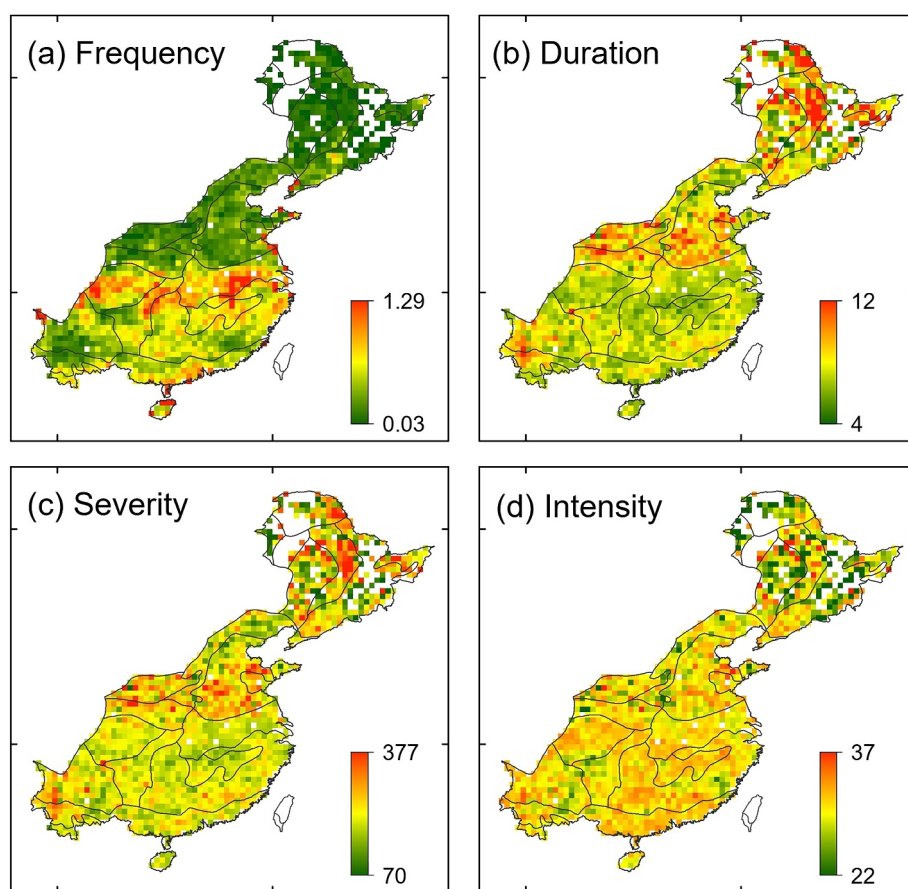


Figure 4. The spatial pattern of the characteristics of flash droughts from 1980 to 2018. Average (a) frequency (unit: times per year), (b) duration (unit: pentad), (c) severity, and (d) intensity of flash drought events. Note: Both severity and intensity are dimensionless.

challenges. To gain a deeper insight into the complex dynamics of flash drought mechanisms, XAI could be a beneficial tool (Tyagi et al., 2022).

3.3. Mechanisms of Flash Drought Onset and Their Patterns

Subsequently, we investigated the spatial and temporal patterns observed from the identified clusters. Figure 6 shows the temporal patterns of the identified four clusters alongside their spatial patterns. Cluster 1 (hereafter referred to as the “Concurrent Prec type”), accounts for 36.8% of total drought pentads, indicating that a concurrent rainfall deficit was the most prominent contributor to drought onset. Within this cluster, precipitation deficit contributed to approximately 50% of drought onset (Figure 6a). Furthermore, it is noteworthy that concurrent high transpiration played a significant role, contributing to approximately 20% of the drought's onset (Figure 6a). The analyses of spatial patterns revealed that concurrent Prec type predominantly manifested in southern China (Figures 6c and 7), characterized by prevailing subtropical and humid climatic conditions (Table S1 in Supporting Information S1).

The Antecedent-concurrent Prec type (Cluster 2), comprises 24.2% of all drought pentads, indicating that the primary factor driving drought is deficits in both antecedent and concurrent precipitation. Precipitation anomalies during these periods contributed significantly to the onset of drought, with approximately 35% attributed to the antecedent period and 30% to the concurrent period. Clusters 1 and 2 suggest that a precipitation shortage can induce soil moisture depletion in a short period (Mo & Lettenmaier, 2016). Additionally, antecedent transpiration and temperature showed approximately non-negligible effects, accounting for about 15% and 10% of the overall contribution, respectively (Figure 6b). Cluster 3 (denoting Antecedent Tem-concurrent Prec type), constituting 19.6% of all drought pentads, underscored the significance of antecedent high temperature and concurrent rainfall

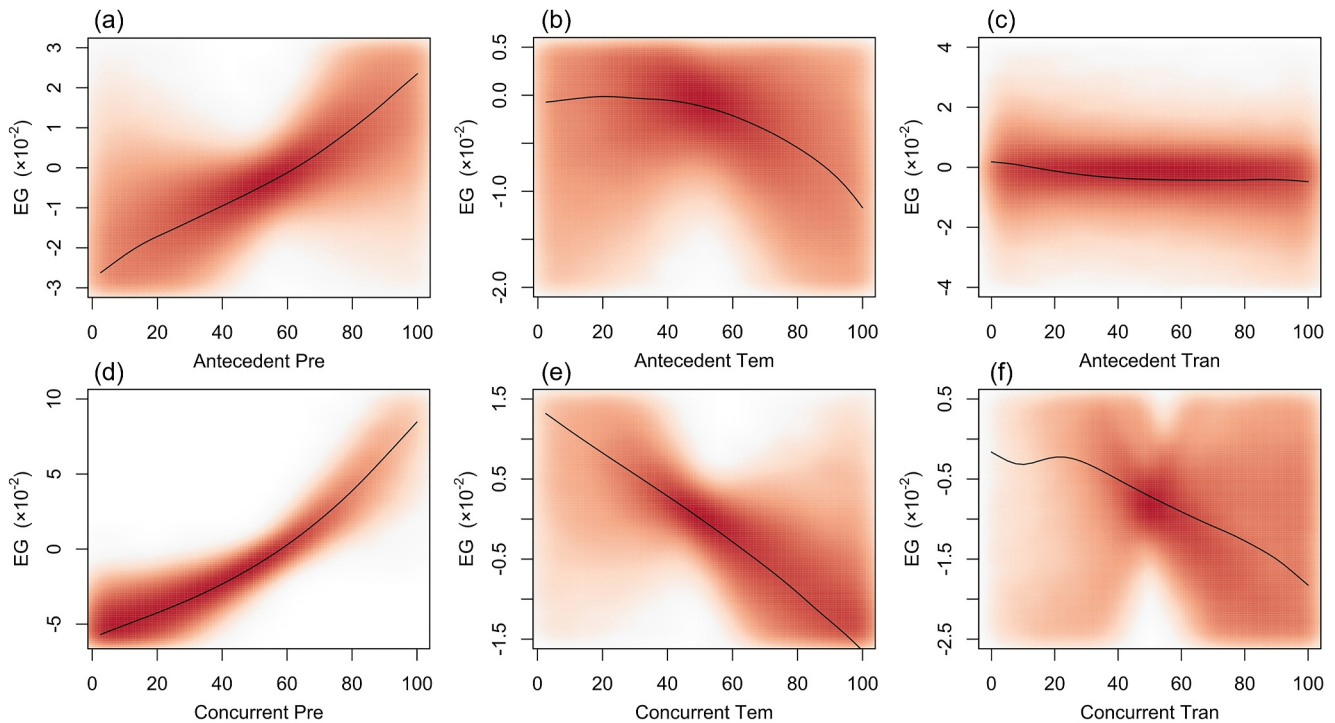


Figure 5. Smoothed scatter plots between the percentile values (%) of drivers and their corresponding expected gradients values across the study region. The solid lines are fitted by the spline function.

deficit. The identification of this mechanism indicates that a high temperature anomaly can swiftly deplete soil moisture, triggering a flash drought, in line with prior studies (Mo & Lettenmaier, 2015; M. Wang et al., 2023). These factors contribute substantially, with roughly 35% and 30% of effects, respectively (Figure 6e). Antecedent-concurrent Prec type predominantly occurred in the southwest and central part of the study region and scattered in northeastern regions, while the Antecedent Tem-concurrent Prec type is primarily observed in northeastern China (Figures 6d and 6g). These regions, except for the central area, are characterized by humid climatic conditions (Figure S5a, Table S1 in Supporting Information S1). The results suggest that the antecedent effects of drivers (specifically, precipitation deficit and high temperature anomaly) play an essential role in flash drought occurrences, particularly in humid regions.

Interestingly, the Antecedent Tran-concurrent Prec type (Cluster 4), accounting for 19.4% of total drought pentads, exhibited a complex temporal pattern. Specifically, antecedent transpiration and concurrent rainfall deficit served as significant contributors to flash drought occurrences, accounting for approximately 35% and 30% of the onset, respectively. Furthermore, concurrent high transpiration also showed indispensable effects, contributing roughly 15% to drought onset (Figure 6f). This mechanism identification suggests that enhanced transpiration, coupled with precipitation deficit, can rapidly deplete soil moisture in the context of climate change (M. Li et al., 2022). Antecedent Tran-concurrent Prec type primarily occurred in northern and northeastern China (Figures 6h and 7), characterized by a predominantly semi-humid climate (Figure S5a in Supporting Information S1). The Cluster 4 highlights the impact of vegetation water consumption, which is revealed to be the dominant mechanism of flash drought in certain regions (M. Li et al., 2022).

Overall, the combined proportion of Cluster 1 and Cluster 2 exceeds 60% and the two clusters show primary contributions of antecedent and concurrent rainfall deficit. In line with previous studies (Koster et al., 2019; Mo & Lettenmaier, 2016), the results highlighted the pivotal role of rainfall deficit in flash drought development. A majority of flash drought onsets (Clusters 2–4), amounting to 63.23% of the total pentads, are closely associated with antecedent conditions. This underscores the complex cumulative effects of factors driving flash drought. In addition, the proportions of Clusters 2–4 are higher in the summer than in autumn (Figures S5c and S5d in Supporting Information S1), indicating that the antecedent impact of drivers on flash drought is prone to be found in humid seasons (Q. Zhu & Wang, 2021). Moreover, Clusters 2 and 3 dominate the humid regions in

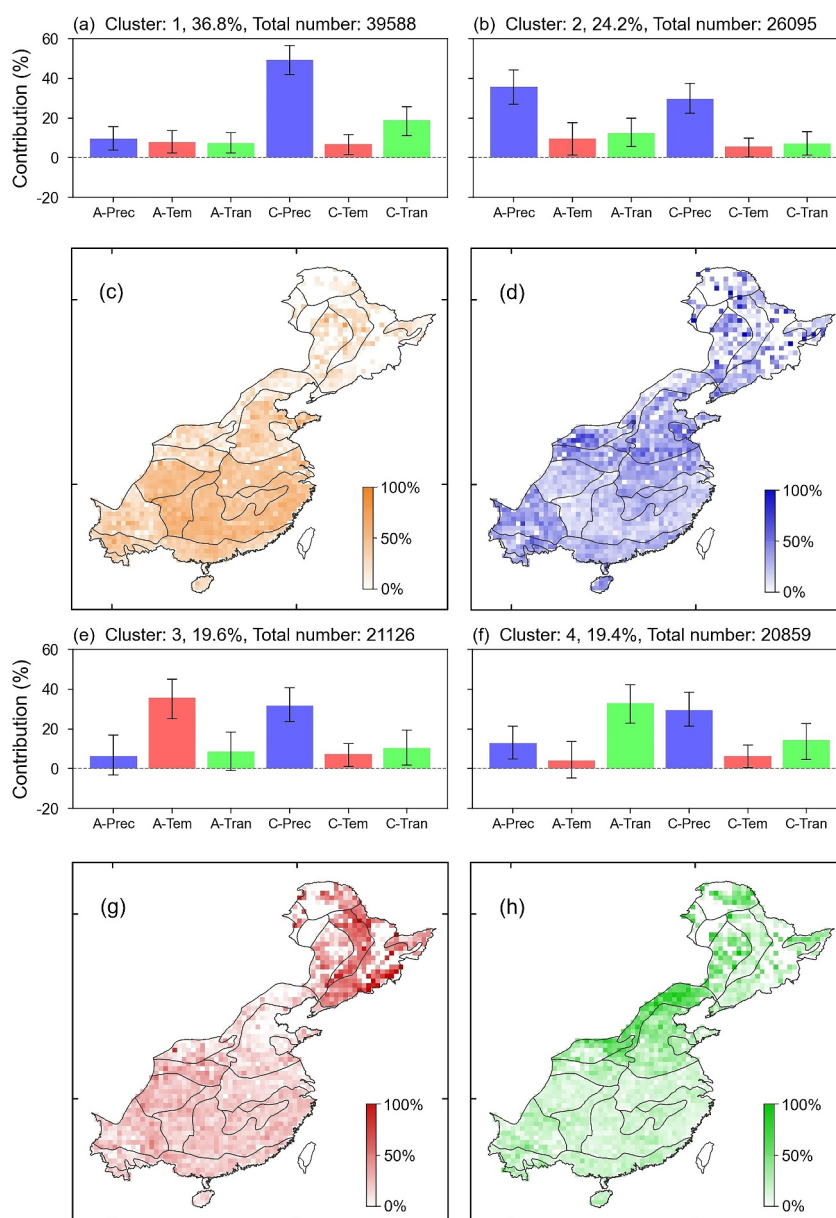


Figure 6. The four types of contribution vectors identified by cluster analysis, presented as normalized contributions: (a) the Concurrent Prec type, (b) the Antecedent-concurrent Prec type, (e) the Antecedent Tem-concurrent Prec type, and (f) the Antecedent Tran-concurrent Prec type. The spatial pattern of proportions of four identified mechanisms: (c) Concurrent Prec type, (d) Antecedent-concurrent Prec type, (g) Antecedent Tem-concurrent Prec type and (h) Antecedent Tran-concurrent Prec type. Note: “A” and “C” on the horizontal axes represent antecedent and concurrent periods, respectively.

southwestern and northeastern China. These findings indicate that in humid regions and seasons, elevated soil moisture levels require an extended duration of antecedent precipitation deficits, high temperature anomalies, or high transpiration anomalies for flash drought onset (Q. Zhu & Wang, 2021). Additionally, Cluster 4, which denotes the importance of antecedent transpiration for flash drought occurrence, was mainly found in semi-humid climate zones. L. Chen et al. (2021) have found a possible association between vegetation water consumption and flash drought occurrences in arid or semi-arid regions. In regions with lower precipitation, latent heat flux is more prone to enhance due to an increased leaf area coverage, consequently leading to diminished soil moisture (L. Chen et al., 2021; Forzieri et al., 2018; Williams & Torn, 2015). Therefore, in those semi-humid regions of northern China, vegetation water consumption plays a more important role in flash drought occurrences.

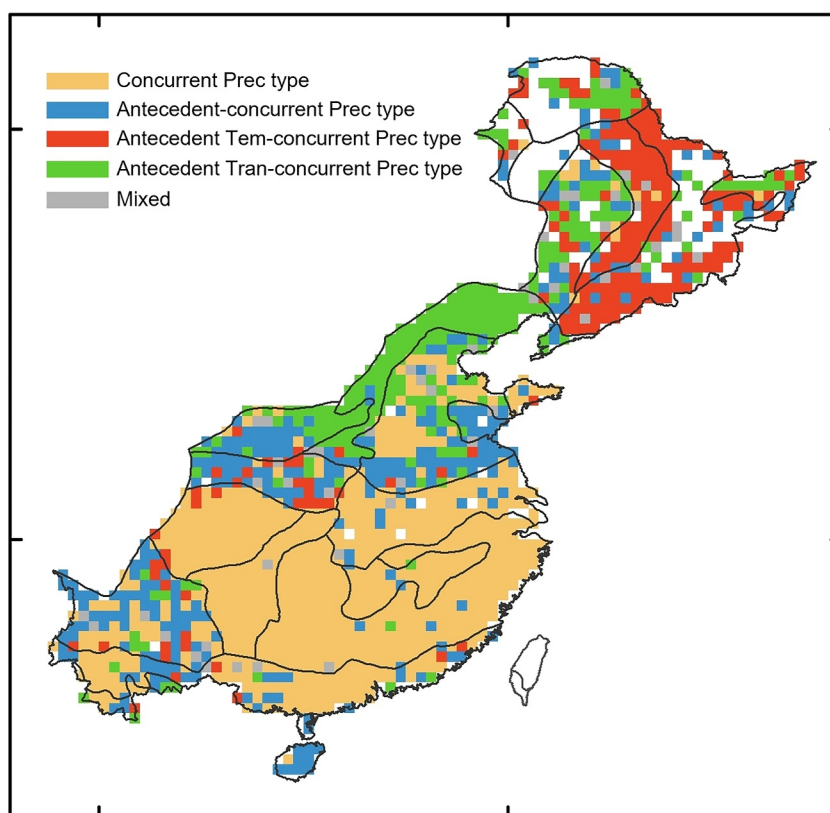


Figure 7. The dominant flash drought mechanism in study area. The dominant clusters were determined based on the cluster with the largest proportion within each grid cell. In instances where multiple clusters exhibited the largest proportion, a grid cell was deemed to be influenced by a mixture of mechanisms.

In addition, to analyze the impact of flash drought detection method on our results, we conducted two additional experiments using methodologies proposed by Ford and Labosier (2017) and Qing et al. (2022), yielding generally similar results (Figures S6 and S7 in Supporting Information S1). However, while strong effects of transpiration were also found in Cluster 4, its contribution was outweighed by concurrent and antecedent precipitation, respectively (Figures S6f and S7f in Supporting Information S1). This inconsistency between methods might be due to the different responses of soil moisture changes to vegetation water consumption. Therefore, enhancing the observation of transpiration during droughts and reducing uncertainty in transpiration data is crucial to improving the robustness of studies related to vegetation water uptake (Coenders-Gerrits et al., 2014). Moreover, we also analyze the impacts of input variables on the identified clusters by conducting experiments using Prec, maximum temperature (T_{\max}), Tran, WS, and RH, resulting in generally consistent outcomes (Figure S8 in Supporting Information S1). Notably, the contribution of T_{\max} closely aligns with the contribution of mean temperature (Figure S8e in Supporting Information S1 and Figure 6e). RH exhibits minor contributions in Cluster 3 and 4, while the contribution of WS is minimal (Figures S8e and S8f in Supporting Information S1). The limited influence of RH and WS may be due to their indirect effects on soil moisture through processes like evaporation and transpiration (Davarzani et al., 2014; Thut, 1938). Overall, the outcomes from the supplementary experiments affirm the robustness of both the flash drought identification method and variable selection employed in this study.

3.4. Spatio-Temporal Evolution of Mechanisms of Flash Drought Onset

To further investigate changes in the driving factors of flash droughts, we conducted a trend analysis for the four types of driving mechanisms (Figure 8a). We first calculated the annual proportions of the four identified flash drought mechanisms across the whole study region during 1980–2018. Then, the temporal evolution of the proportions of four drought mechanisms was investigated with the Theil-Sen estimator (Sen, 1968; Theil, 1992).

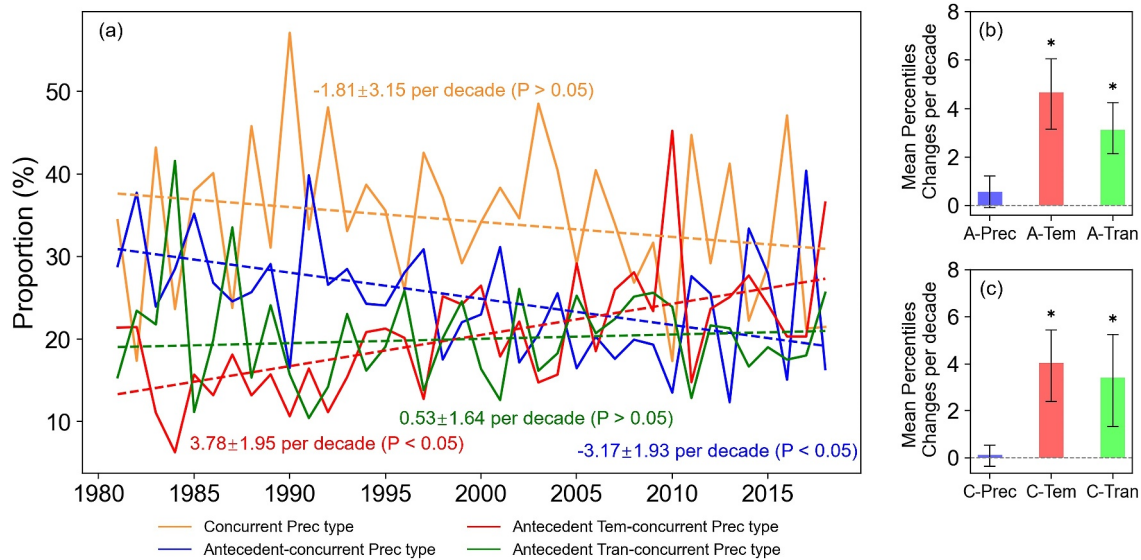


Figure 8. (a) Temporal evolution of four identified drought mechanisms across the whole study regions. Dashed lines represent trend slopes calculated using Theil-Sen estimator. (b) Trends in mean percentiles of potential flash drought drivers during antecedent periods, as calculated with Theil-Sen estimator. Panel (c) Same as panel (b), but for drivers during concurrent periods. Asterisks in (b) and (c) denote drivers with significant trends ($P < 0.05$). In panels (b, c), we first transformed the values of drivers (Prec, Tem, and Tran) into percentiles to maintain consistency with the format of soil moisture data. Then, we computed the mean values of each driver during the antecedent and concurrent periods of flash drought events. Subsequently, we performed trend analysis using the Theil-Sen estimator to ascertain the trends of the drivers and assess the significance of these trends.

The results unveiled statistically significant declining trends ($P < 0.05$) for the Antecedent-concurrent Prec type and a non-significant declining trend for the Concurrent Prec type, suggesting a diminishing role of rainfall in flash drought onset (Figure 8a). Correspondingly, both antecedent and concurrent Prec exhibit an increase (Figures 8b and 8c). This suggests that an increase in precipitation across the study area may contribute to a reduced impact of rainfall deficit on flash drought occurrence (Liu et al., 2015; Sun & Ao, 2013).

Conversely, along with a significant increase of temperature and a non-significant increase of precipitation during the antecedent period of droughts (Figure 8b), the Antecedent Tem-concurrent Prec type exhibited a significant increasing trend (Figure 8a). These results are consistent with previous studies (Noguera et al., 2022; Shah et al., 2022), implying an escalating influence of antecedent high temperature in fostering the occurrence of flash droughts under global warming (Christian et al., 2023). Furthermore, in conjunction with the sustained increase in positive transpiration anomalies (Figures 8b and 8c), the Antecedent Tran-concurrent Prec type exhibited an intensified trend (Figure 8a). This trend implies a potential amplification of vegetation water consumption's role in influencing the occurrence of flash droughts (Guo et al., 2023). These results imply a growing influence of antecedent conditions, particularly antecedent temperature and transpiration (Shah et al., 2023).

Subsequently, we analyzed the spatial patterns of trends for each identified cluster with a 15-year moving window (Figure 9). The findings indicate a substantial decreasing trend in both the Concurrent Prec type and the Antecedent-concurrent Prec type across the predominant part of the study area, particularly in southern China (Figure 9a). This aligns with the noteworthy increase in precipitation observed in the southern region (Q. Zhang et al., 2011). In contrast, Antecedent Tem-concurrent Prec exhibited widespread increased trends respectively across study regions (Figures 9b and 9c). These shifts suggest that the occurrence of flash droughts solely driven by concurrent Prec deficit could be diminishing under climate change, while the influence of antecedent conditions on flash drought onset could become increasingly important across northern China (M. Zhang et al., 2022). Moreover, the Antecedent Tran-concurrent Prec type exhibited a complex spatial pattern, characterized by a substantial upward trend in most of the southeastern and northeastern regions, which predominantly comprise humid areas (Figure 9d). In contrast, it showed a significant decreasing trend in northern and northwestern regions, which are primarily semi-humid regions. The result suggests an escalating role of vegetation water consumption in shaping soil moisture flash drought onset in humid areas, aligning with the study of Guo et al. (2023).

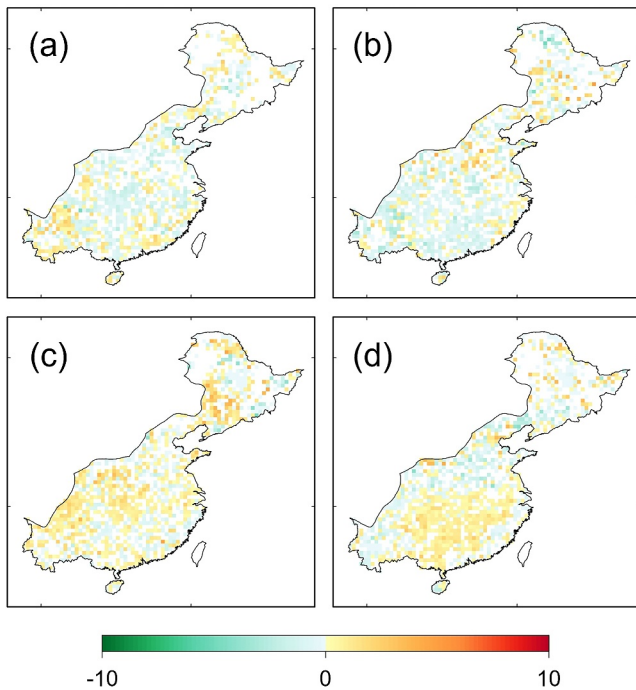


Figure 9. The spatial pattern of trends associated with different mechanisms (unit: percent per year). (a) Concurrent Prec type, (b) Antecedent-concurrent Prec type, (c) Antecedent Tem-concurrent Prec type and (d) Antecedent Tran-concurrent Prec type. The trends were calculated with a 15-year moving window. Only the grid cells with significant trend ($P < 0.05$) were plotted.

Additionally, we performed similar analyses using 10-year and 20-year moving windows, yielding similar results (Figure S9 in Supporting Information S1). Taken together, our analyses imply a potentially escalated influence of high temperature and vegetation water consumption on flash drought onsets, paralleled by an increasing significance of antecedent conditions. The temporal analysis provides valuable insights into the dynamic nature of flash drought mechanisms, thereby enhancing our understanding of their evolving impact on flash drought occurrences.

3.5. Classification of Flash Drought Events

To gain more insights into the underlying mechanisms shaping an individual flash drought event, a categorization of various types of flash drought events was conducted in this section. We first calculated the proportions of different types of mechanisms within the pentads in each flash drought event. Subsequently, the preeminent types of mechanisms served as the basis for classifying each specific flash drought event. Figure 10 illustrates the proportions of identified flash drought event types. Upon employing the relatively low threshold (60%) for classification, the results revealed that the top four event types with the largest proportion were predominantly driven by one main mechanism (Figure 10b). However, upon implementing higher thresholds (i.e., 75% and 85%) for the classification, the results indicated that several of the major event types were linked with a convergence of multiple mechanisms (Figures 10a–10c). Moreover, in comparison to the results obtained with the 60% threshold, the classifications generated using the two higher thresholds exhibited greater stability. These classifications revealed the intricate time-varying pattern of flash drought events associated with multiple mechanisms.

We next used the results based on the 75% threshold for further investigation (Figure 10a). All events can be classified into 15 distinct categories, and roughly 70% of the events are driven by at least two mechanisms, underscoring the multifaced nature of flash drought event drivers. Notably, the majority of events were associated with the Antecedent-concurrent Prec type (Cluster 2), the Antecedent Tem-concurrent Prec type (Cluster 3), or the Antecedent Tran-concurrent Prec type (Cluster 4). This emphasizes the pronounced influence of antecedent conditions in shaping the dynamics of flash drought occurrences (Shah et al., 2023). In addition, some flash drought events were only driven by the Concurrent Prec type (Cluster 1), indicating the crucial role of concurrent Prec deficit in flash drought occurrences (Koster et al., 2019).

We also analyzed the spatial patterns of the identified types of drought event mechanisms. Figure 11 shows the nine most prevalent types, and the remaining types are presented in Figure S10 in Supporting Information S1. The results showed that the spatial distribution of events driven by a single mechanism (Figures 11d–11g) exhibited similar patterns to those shown in Figures 6a–6d. Additionally, events driven by multiple mechanisms showed clear spatial patterns. Specifically, flash drought events linked to the Antecedent-concurrent Prec type and the Antecedent-concurrent Prec type were predominantly prevalent in southwestern China (Figure 11a). Meanwhile, events related to the Concurrent Prec type and Antecedent Tem-concurrent Prec type were mainly observed in northeastern China (Figure 11b). Furthermore, events associated with the Concurrent Prec type and Antecedent Tran-concurrent Prec type were dominant in the central part of the study region (Figure 11c). Overall, these results suggest more diverse mechanisms for flash drought events in these regions. This circumstance could potentially pose greater challenges in terms of prediction and mitigation efforts for flash drought events (Shah et al., 2022; M. Zhang et al., 2022). Consequently, heightened attention may be warranted for these specific regions.

In summary, we presented a comprehensive classification of flash drought events and examined their spatial patterns by analyzing the composition of mechanisms within the individual events. We overall identified 15 different types of flash drought events, and a majority of them (about 70%) were driven by multiple drivers, underscoring the complex time-varying patterns of flash drought events.

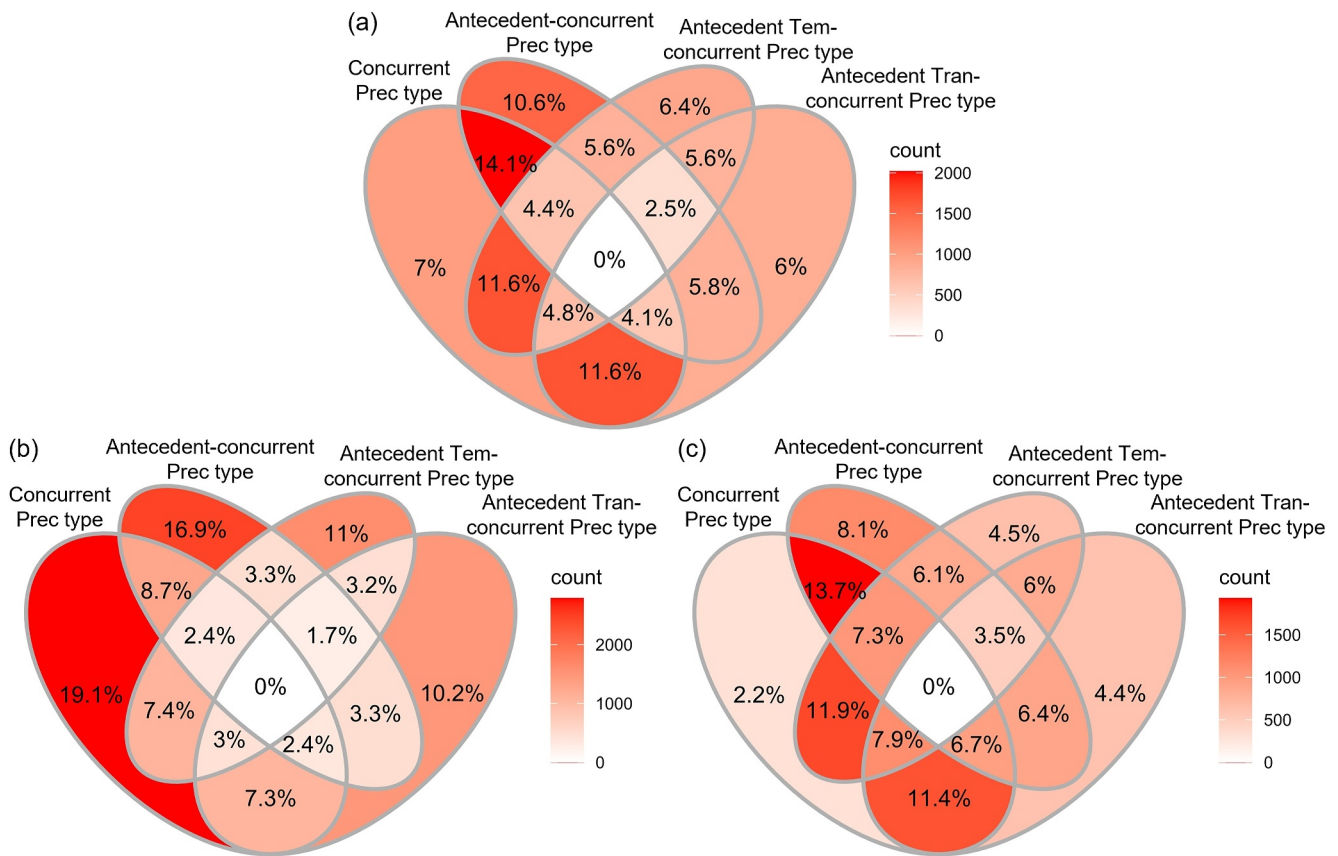


Figure 10. Venn diagrams that show the percentages and total counts of flash drought event types associated with different mechanisms based on the (a) 75%, (b) 60%, and (c) 85% threshold. The intersections of the Venn diagrams indicate the proportions of these flash drought events driven by multiple identified mechanisms. Note: Flash drought events classified as mixed mechanism are not shown in this figure due to their scarcity.

4. Conclusion

To enhance our understanding of the driving mechanisms of flash droughts and their changes for effective drought management and adaptation strategies, this study introduces a novel framework to investigate the mechanisms of flash droughts and their changes in eastern China by using the cutting-edge explainable artificial intelligence approach.

The results of the study reveal that (a) the Concurrent Prec type is the most prevalent type (accounting for 36.8% of all pentads), mainly occurring in southern China. (b) 19.4% of drought onsets were linked to the Antecedent Tran-concurrent Prec type, which prevails in semi-humid regions, underscoring the non-neglectable contribution of vegetation water consumption to flash droughts. (c) 63.23% of drought onsets exhibited close association with the antecedent conditions, with the antecedent anomalies contributing approximately 50% of overall effects, which highlights the importance of the cumulative effects of drivers in flash drought occurrences. (d) The subsequent trend analyses showed that the driving mechanisms associated with the anomalies in temperature and transpiration displayed an obvious increase, paralleled by an increasing significance of antecedent conditions. Such results imply a potentially escalated influence of high temperature and vegetation water consumption on flash drought onsets. (e) The classification of flash drought events based on the different types of driving mechanisms indicates that all flash drought events in the study region can be classified into 15 types and around 70% of flash drought events were driven by at least two types of driving mechanisms, indicating a complex time-varying pattern of driving factors during flash drought events.

In summary, this study contributes to the scientific understanding of the underlying mechanisms driving flash droughts and provides valuable insights for drought management and water resource planning in China. Moreover, this study presents a comprehensive framework that not only facilitates the exploration and interpretation of

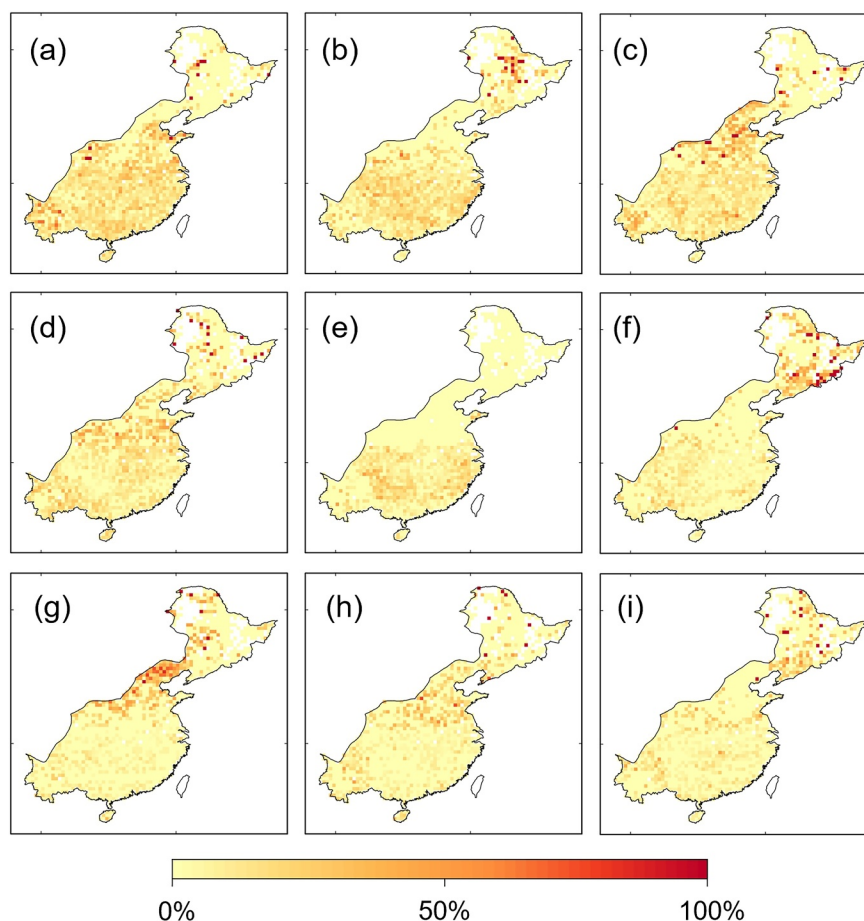


Figure 11. The percentage of spatial patterns corresponding to the top nine types of flash drought events associated with different mechanisms. Events driven by (a) the Concurrent Prec type and the Antecedent-concurrent Prec type, (b) the Concurrent Prec type and the Antecedent Tem-concurrent Prec type, (c) the Concurrent Prec type and the Antecedent Tran-concurrent Prec type, (d) the Antecedent-concurrent Prec type, (e) the Concurrent Prec type, (f) the Antecedent Tem-concurrent Prec type, (g) the Antecedent Tran-concurrent Prec type, (h) the Antecedent-concurrent Prec type and the Antecedent Tran-concurrent Prec type, and (i) the Antecedent-concurrent Prec type and the Antecedent Tem-concurrent Prec type.

the multifaceted mechanisms of flash droughts within China but also potentially extends its relevance to broader geographical contexts.

Data Availability Statement

The soil moisture and transpiration datasets from the Global Land Evaporation Amsterdam Model are publicly available from Martens et al. (2017) and Miralles et al. (2011), and the specific download link is <https://www.gleam.eu/>; the precipitation, mean air temperature, relative humidity, and wind speed data sets are obtained from the China Meteorological Administration, which is described in J. Li et al. (2021) and can be downloaded from <https://data.cma.cn/data/detail/dataCode/A.0012.0001.S011.html>.

The establishment of the LSTM models was performed using TensorFlow (Abadi et al., 2015) and Keras (Chollet, 2015), and the interpretability analysis was performed using SHAP (Lundberg & Lee, 2017). Software for this research is available in GitHub (TensorFlow: <https://github.com/tensorflow/tensorflow>; Keras: <https://github.com/keras-team/keras>; SHAP: <https://github.com/shap/shap>).

Acknowledgments

We would like to thank the editors and anonymous reviewers for their detailed and constructive comments, which helped to significantly improve the manuscript. This research was financially supported by the National Natural Science Foundation of China (52109019), the Guangdong Basic and Applied Basic Research Foundation (2023B1515020087, 2023A1515030191, 2021A1515010935), and the cooperation research project between South China University of Technology and Qingyuan Hydrology Sub-bureau of Guangdong Province (QYSWFK-2022-85). J.L. acknowledges the National Natural Science Foundation of China (42301106). S.J. acknowledges support by the Carl Zeiss Stiftung. Z.Z. acknowledges the National Natural Science Foundation of China (52209019) and the Guangzhou Basic and Applied Basic Research Scheme (2023A04J1595).

References

- Abadi, M., Agarwal, A., Barham, P., Brevdo, E., Chen, Z., Citro, C., et al. (2015). TensorFlow: Large-scale machine learning on heterogeneous systems [Software]. *Zenodo*. <https://doi.org/10.5281/zenodo.10794955>
- Ahmad, S. K., Kumar, S. V., Lahmers, T. M., Wang, S., Liu, P.-W., Wrzesien, M. L., et al. (2022). Flash drought onset and development mechanisms captured with soil moisture and vegetation data assimilation. *Water Resources Research*, *58*(12), e2022WR032894. <https://doi.org/10.1029/2022WR032894>
- Basara, J. B., Christian, J. I., Wakefield, R. A., Otkin, J. A., Hunt, E. H., & Brown, D. P. (2019). The evolution, propagation, and spread of flash drought in the Central United States during 2012. *Environmental Research Letters*, *14*(8), 084025. <https://doi.org/10.1088/1748-9326/ab2cc0>
- Boyer, J. S., Byrne, P., Cassman, K. G., Cooper, M., Delmer, D., Greene, T., et al. (2013). The U.S. Drought of 2012 in perspective: A call to action. *Global Food Security*, *2*(3), 139–143. <https://doi.org/10.1016/j.gfs.2013.08.002>
- Chen, L., Ford, T. W., & Yadav, P. (2021). The role of vegetation in flash drought occurrence: A sensitivity study using community earth system model, version 2. *Journal of Hydrometeorology*, *22*(4), 845–857. <https://doi.org/10.1175/JHM-D-20-0214.1>
- Chen, L. G., Gottschalck, J., Hartman, A., Miskus, D., Tinker, R., & Artusa, A. (2019). Flash drought characteristics based on U.S. Drought monitor. *Atmosphere*, *10*(9), 498. <https://doi.org/10.3390/atmos10090498>
- Chollet, F. (2015). Keras: Deep learning for humans [Software]. *Keras*. Retrieved from <https://keras.io>
- Christian, J. I., Basara, J. B., Otkin, J. A., Hunt, E. D., Wakefield, R. A., Flanagan, P. X., & Xiao, X. (2019). A methodology for flash drought identification: Application of flash drought frequency across the United States. *Journal of Hydrometeorology*, *20*(5), 833–846. <https://doi.org/10.1175/JHM-D-18-0198.1>
- Christian, J. I., Martin, E. R., Basara, J. B., Furtado, J. C., Otkin, J. A., Lowman, L. E. L., et al. (2023). Global projections of flash drought show increased risk in a warming climate. *Communications Earth & Environment*, *4*(1), 165. <https://doi.org/10.1038/s43247-023-00826-1>
- Coenders-Gerrits, A. M. J., Van Der Ent, R. J., Bogaard, T. A., Wang-Erlandsson, L., Hrachowitz, M., & Savenije, H. H. G. (2014). Uncertainties in transpiration estimates. *Nature*, *506*(7487), E1–E2. <https://doi.org/10.1038/nature12925>
- Cook, B. I., Mankin, J. S., Marvel, K., Williams, A. P., Smerdon, J. E., & Anchukaitis, K. J. (2020). Twenty-first century drought projections in the CMIP6 forcing scenarios. *Earth's Future*, *8*(6), e2019EF001461. <https://doi.org/10.1029/2019EF001461>
- Davarzani, H., Smits, K., Tolene, R. M., & Illangasekare, T. (2014). Study of the effect of wind speed on evaporation from soil through integrated modeling of the atmospheric boundary layer and shallow subsurface. *Water Resources Research*, *50*(1), 661–680. <https://doi.org/10.1002/2013WR013952>
- Dikshit, A., & Pradhan, B. (2021a). Explainable AI in drought forecasting. *Machine Learning with Applications*, *6*, 100192. <https://doi.org/10.1016/j.mlwa.2021.100192>
- Dikshit, A., & Pradhan, B. (2021b). Interpretable and explainable AI (XAI) model for spatial drought prediction. *Science of the Total Environment*, *801*, 149797. <https://doi.org/10.1016/j.scitotenv.2021.149797>
- Ding, Y., Zhu, Y., Feng, J., Zhang, P., & Cheng, Z. (2020). Interpretable spatio-temporal attention LSTM model for flood forecasting. *Neurocomputing*, *403*, 348–359. <https://doi.org/10.1016/j.neucom.2020.04.110>
- Erion, G., Janizek, J. D., Sturmfels, P., Lundberg, S. M., & Lee, S.-I. (2021). Improving performance of deep learning models with axiomatic attribution priors and expected gradients. *Nature Machine Intelligence*, *3*(7), 620–631. <https://doi.org/10.1038/s42256-021-00343-w>
- Ford, T. W., & Labosier, C. F. (2017). Meteorological conditions associated with the onset of flash drought in the Eastern United States. *Agricultural and Forest Meteorology*, *247*, 414–423. <https://doi.org/10.1016/j.agrformet.2017.08.031>
- Forgy, E. W. (1965). Cluster analysis of multivariate data: Efficiency versus interpretability of classifications. *Biometrics*, *21*, 768–780.
- Forzieri, G., Duveiller, G., Georgievski, G., Li, W., Robertson, E., Kautz, M., et al. (2018). Evaluating the interplay between biophysical processes and leaf area changes in land surface models. *Journal of Advances in Modeling Earth Systems*, *10*(5), 1102–1126. <https://doi.org/10.1002/2018MS001284>
- Fu, R., Zhang, Z., & Li, L. (2016). Using LSTM and GRU neural network methods for traffic flow prediction. In *2016 31st Youth academic annual conference of Chinese association of automation (YAC)* (pp. 324–328). IEEE. <https://doi.org/10.1109/YAC.2016.7804912>
- Grigg, N. S. (2014). The 2011–2012 drought in the United States: New lessons from a record event. *International Journal of Water Resources Development*, *30*(2), 183–199. <https://doi.org/10.1080/07900627.2013.847710>
- Guo, W., Huang, S., Huang, Q., She, D., Shi, H., Leng, G., et al. (2023). Precipitation and vegetation transpiration variations dominate the dynamics of agricultural drought characteristics in China. *Science of the Total Environment*, *898*, 165480. <https://doi.org/10.1016/j.scitotenv.2023.165480>
- Gupta, H. V., Kling, H., Yilmaz, K. K., & Martinez, G. F. (2009). Decomposition of the mean squared error and NSE performance criteria: Implications for improving hydrological modelling. *Journal of Hydrology*, *377*(1–2), 80–91. <https://doi.org/10.1016/j.jhydrol.2009.08.003>
- Hochreiter, S., & Schmidhuber, J. (1997). Long short-term memory. *Neural Computation*, *9*(8), 1735–1780. <https://doi.org/10.1162/neco.1997.9.8.1735>
- Jiang, S., Zheng, Y., Wang, C., & Babovic, V. (2022). Uncovering flooding mechanisms across the contiguous United States through interpretive deep learning on representative catchments. *Water Resources Research*, *58*(1), e2021WR030185. <https://doi.org/10.1029/2021WR030185>
- Kalma, J. D., McVicar, T. R., & McCabe, M. F. (2008). Estimating land surface evaporation: A review of methods using remotely sensed surface temperature data. *Surveys in Geophysics*, *29*(4), 421–469. <https://doi.org/10.1007/s10712-008-9037-z>
- Karpatne, A., Ebert-Uphoff, I., Ravela, S., Babaie, H. A., & Kumar, V. (2019). Machine learning for the geosciences: Challenges and opportunities. *IEEE Transactions on Knowledge and Data Engineering*, *31*(8), 1544–1554. <https://doi.org/10.1109/TKDE.2018.2861006>
- Kling, H., Fuchs, M., & Paulin, M. (2012). Runoff conditions in the upper Danube basin under an ensemble of climate change scenarios. *Journal of Hydrology*, *424–425*, 264–277. <https://doi.org/10.1016/j.jhydrol.2012.01.011>
- Koster, R. D., Schubert, S. D., Wang, H., Mahanama, S. P., & DeAngelis, A. M. (2019). Flash drought as captured by reanalysis data: Disentangling the contributions of precipitation deficit and excess evapotranspiration. *Journal of Hydrometeorology*, *20*(6), 1241–1258. <https://doi.org/10.1175/JHM-D-18-0242.1>
- Kratzert, F., Klotz, D., Brenner, C., Schulz, K., & Herrnegger, M. (2018). Rainfall–runoff modelling using Long Short-Term Memory (LSTM) networks. *Hydrology and Earth System Sciences*, *22*(11), 6005–6022. <https://doi.org/10.5194/hess-22-6005-2018>
- Kuwayama, Y., Thompson, A., Bernknopf, R., Zaitchik, B., & Vail, P. (2019). Estimating the impact of drought on agriculture using the U.S. Drought monitor. *American Journal of Agricultural Economics*, *101*(1), 193–210. <https://doi.org/10.1093/ajae/aaay037>
- Li, J., Bevacqua, E., Chen, C., Wang, Z., Chen, X., Myneni, R. B., et al. (2022). Regional asymmetry in the response of global vegetation growth to springtime compound climate events. *Communications Earth & Environment*, *3*(1), 123. <https://doi.org/10.1038/s43247-022-00455-0>
- Li, J., Bevacqua, E., Wang, Z., Sitch, S., Arora, V., Arneeth, A., et al. (2023). Hydroclimatic extremes contribute to asymmetric trends in ecosystem productivity loss. *Communications Earth & Environment*, *4*(1), 1–10. <https://doi.org/10.1038/s43247-023-00869-4>

- Li, J., Wang, Z., Wu, X., c, C.-Y., Guo, S., & Chen, X. (2020). Toward monitoring short-term droughts using a novel daily scale, standardized antecedent precipitation evapotranspiration index. *Journal of Hydrometeorology*, 21(5), 891–908. <https://doi.org/10.1175/JHM-D-19-0298.1>
- Li, J., Wang, Z., Wu, X., Chen, J., Guo, S., & Zhang, Z. (2020). A new framework for tracking flash drought events in space and time. *CATENA*, 194, 104763. <https://doi.org/10.1016/j.catena.2020.104763>
- Li, J., Wang, Z., Wu, X., Zscheischler, J., Guo, S., & Chen, X. (2021). A standardized index for assessing sub-monthly compound dry and hot conditions with application in China [Dataset]. *Hydrology and Earth System Sciences*, 25(3), 1587–1601. <https://doi.org/10.5194/hess-25-1587-2021>
- Li, M., Wu, P., Ma, Z., Pan, Z., Lv, M., Yang, Q., & Duan, Y. (2022). The increasing role of vegetation transpiration in soil moisture loss across China under global warming. *Journal of Hydrometeorology*, 23(2), 253–274. <https://doi.org/10.1175/JHM-D-21-0132.1>
- Li, P., Jia, L., Lu, J., Jiang, M., & Zheng, C. (2024). A new evapotranspiration-based drought index for flash drought identification and monitoring. *Remote Sensing*, 16(5), 780. <https://doi.org/10.3390/rs16050780>
- Li, S., Liang, W., Zhang, W., & Liu, Q. (2016). Response of soil moisture to hydro-meteorological variables under different precipitation gradients in the Yellow river basin. *Water Resources Management*, 30(6), 1867–1884. <https://doi.org/10.1007/s11269-016-1244-7>
- Li, S., & Sawada, Y. (2022). Soil moisture-vegetation interaction from near-global in-situ soil moisture measurements. *Environmental Research Letters*, 17(11), 114028. <https://doi.org/10.1088/1748-9326/ac9c1f>
- Li, W., Migliavacca, M., Forkel, M., Denissen, J. M. C., Reichstein, M., Yang, H., et al. (2022). Widespread increasing vegetation sensitivity to soil moisture. *Nature Communications*, 13(1), 3959. <https://doi.org/10.1038/s41467-022-31667-9>
- Lian, X., Piao, S., Huntingford, C., Li, Y., Zeng, Z., Wang, X., et al. (2018). Partitioning global land evapotranspiration using CMIP5 models constrained by observations. *Nature Climate Change*, 8(7), 640–646. <https://doi.org/10.1038/s41558-018-0207-9>
- Linardatos, P., Papastefanopoulos, V., & Kotsiantis, S. (2020). Explainable AI: A review of machine learning interpretability methods. *Entropy*, 23(1), 18. <https://doi.org/10.3390/e23010018>
- Lisonbee, J., Woloszyn, M., & Skumanich, M. (2021). Making sense of flash drought: Definitions, indicators, and where we go from here. *Journal of Applied and Service Climatology*, 2021(1), 1–19. <https://doi.org/10.46275/JOASC.2021.02.001>
- Liu, R., Liu, S. C., Cicerone, R. J., Shiu, C.-J., Li, J., Wang, J., & Zhang, Y. (2015). Trends of extreme precipitation in eastern China and their possible causes. *Advances in Atmospheric Sciences*, 32(8), 1027–1037. <https://doi.org/10.1007/s00376-015-5002-1>
- Lundberg, S., & Lee, S.-I. (2017). A unified approach to interpreting model predictions [Software]. *arXiv*. Retrieved from <http://arxiv.org/abs/1705.07874>
- Mahto, S. S., & Mishra, V. (2023). Increasing risk of simultaneous occurrence of flash drought in major global croplands. *Environmental Research Letters*, 18(4), 044044. <https://doi.org/10.1088/1748-9326/acc8ed>
- Mamalakis, A., Ebert-Uphoff, I., & Barnes, E. A. (2022). Explainable artificial intelligence in meteorology and climate science: Model fine-tuning, calibrating trust and learning new science. In A. Holzinger, R. Goebel, R. Fong, T. Moon, K.-R. Müller, & W. Samek (Eds.), *XXAI—Beyond explainable AI: International workshop, held in conjunction with ICML 2020, July 18, 2020, Vienna, Austria, revised and extended papers* (pp. 315–339). Springer International Publishing. https://doi.org/10.1007/978-3-031-04083-2_16
- Martens, B., Miralles, D. G., Lievens, H., van der Schalie, R., de Jeu, R. A. M., Fernández-Prieto, D., et al. (2017). GLEAM v3: Satellite-based land evaporation and root-zone soil moisture [Dataset]. *Geoscientific Model Development*, 10(5), 1903–1925. <https://doi.org/10.5194/gmd-10-1903-2017>
- Miralles, D. G., Holmes, T. R. H., De Jeu, R. a. M., Gash, J. H., Meesters, A. G. C. A., & Dolman, A. J. (2011). Global land-surface evaporation estimated from satellite-based observations [Dataset]. *Hydrology and Earth System Sciences*, 15(2), 453–469. <https://doi.org/10.5194/hess-15-453-2011>
- Mo, K. C., & Lettenmaier, D. P. (2015). Heat wave flash droughts in decline: The flash droughts in the U.S. *Geophysical Research Letters*, 42(8), 2823–2829. <https://doi.org/10.1002/2015GL064018>
- Mo, K. C., & Lettenmaier, D. P. (2016). Precipitation deficit flash droughts over the United States. *Journal of Hydrometeorology*, 17(4), 1169–1184. <https://doi.org/10.1175/JHM-D-15-0158.1>
- Mukherjee, S., & Mishra, A. K. (2022). Global flash drought analysis: Uncertainties from indicators and datasets. *Earth's Future*, 10(6), e2022EF002660. <https://doi.org/10.1029/2022EF002660>
- Murdoch, W. J., Singh, C., Kumbier, K., Abbasi-Asl, R., & Yu, B. (2019). Definitions, methods, and applications in interpretable machine learning. *Proceedings of the National Academy of Sciences*, 116(44), 22071–22080. <https://doi.org/10.1073/pnas.1900654116>
- Nash, J. E., & Sutcliffe, J. V. (1970). River flow forecasting through conceptual models part I—A discussion of principles. *Journal of Hydrology*, 10(3), 282–290. [https://doi.org/10.1016/0022-1694\(70\)90255-6](https://doi.org/10.1016/0022-1694(70)90255-6)
- Niu, Z., He, H., Zhu, G., Ren, X., Zhang, L., Zhang, K., et al. (2019). An increasing trend in the ratio of transpiration to total terrestrial evapotranspiration in China from 1982 to 2015 caused by greening and warming. *Agricultural and Forest Meteorology*, 279, 107701. <https://doi.org/10.1016/j.agrformet.2019.107701>
- Noguera, I., Vicente-Serrano, S. M., & Domínguez-Castro, F. (2022). The rise of atmospheric evaporative demand is increasing flash droughts in Spain during the warm season. *Geophysical Research Letters*, 49(11), e2021GL097703. <https://doi.org/10.1029/2021GL097703>
- Otkin, J. A., Anderson, M. C., Hain, C., Svoboda, M., Johnson, D., Mueller, R., et al. (2016). Assessing the evolution of soil moisture and vegetation conditions during the 2012 United States flash drought. *Agricultural and Forest Meteorology*, 218–219, 230–242. <https://doi.org/10.1016/j.agrformet.2015.12.065>
- Otkin, J. A., Svoboda, M., Hunt, E. D., Ford, T. W., Anderson, M. C., Hain, C., & Basara, J. B. (2018). Flash droughts: A review and assessment of the challenges imposed by rapid-onset droughts in the United States. *Bulletin of the American Meteorological Society*, 99(5), 911–919. <https://doi.org/10.1175/BAMS-D-17-0149.1>
- Pendergrass, A. G., Meehl, G. A., Pulwarty, R., Hobbins, M., Hoell, A., AghaKouchak, A., et al. (2020). Flash droughts present a new challenge for subseasonal-to-seasonal prediction. *Nature Climate Change*, 10(3), 191–199. <https://doi.org/10.1038/s41558-020-0709-0>
- Piao, S., Wang, X., Park, T., Chen, C., Lian, X., He, Y., et al. (2020). Characteristics, drivers and feedbacks of global greening. *Nature Reviews Earth & Environment*, 1(1), 14–27. <https://doi.org/10.1038/s43017-019-0001-x>
- Poppe Terán, C., Naz, B. S., Graf, A., Qu, Y., Hendricks Franssen, H.-J., Baatz, R., et al. (2023). Rising water-use efficiency in European grasslands is driven by increased primary production. *Communications Earth & Environment*, 4(1), 1–13. <https://doi.org/10.1038/s43247-023-00757-x>
- Qing, Y., Wang, S., Ancell, B. C., & Yang, Z.-L. (2022). Accelerating flash droughts induced by the joint influence of soil moisture depletion and atmospheric aridity. *Nature Communications*, 13(1), 1139. <https://doi.org/10.1038/s41467-022-28752-4>
- Reichstein, M., Camps-Valls, G., Stevens, B., Jung, M., Denzler, J., Carvalhais, N., & Prabhat (2019). Deep learning and process understanding for data-driven Earth system science. *Nature*, 566(7743), 195–204. <https://doi.org/10.1038/s41586-019-0912-1>

- Roscher, R., Bohn, B., Duarte, M. F., & Garcke, J. (2020). Explainable machine learning for scientific insights and discoveries. *IEEE Access*, 8, 42200–42216. <https://doi.org/10.1109/ACCESS.2020.2976199>
- Rousseeuw, P. J. (1987). Silhouettes: A graphical aid to the interpretation and validation of cluster analysis. *Journal of Computational and Applied Mathematics*, 20, 53–65. [https://doi.org/10.1016/0377-0427\(87\)90125-7](https://doi.org/10.1016/0377-0427(87)90125-7)
- Samek, W., & Müller, K.-R. (2019). Towards explainable artificial intelligence. In W. Samek, G. Montavon, A. Vedaldi, L. K. Hansen, & K.-R. Müller (Eds.), *Explainable AI: Interpreting, explaining and visualizing deep learning* (pp. 5–22). Springer International Publishing. https://doi.org/10.1007/978-3-030-28954-6_1
- Sehler, R., Li, J., Reager, J., & Ye, H. (2019). Investigating relationship between soil moisture and precipitation globally using remote sensing observations. *Journal of Contemporary Water Research & Education*, 168(1), 106–118. <https://doi.org/10.1111/j.1936-704X.2019.03324.x>
- Sen, P. K. (1968). Estimates of the regression coefficient based on Kendall's Tau. *Journal of the American Statistical Association*, 63(324), 1379–1389. <https://doi.org/10.1080/01621459.1968.10480934>
- Shah, J., Hari, V., Rakovec, O., Markonis, Y., Samaniego, L., Mishra, V., et al. (2022). Increasing footprint of climate warming on flash droughts occurrence in Europe. *Environmental Research Letters*, 17(6), 064017. <https://doi.org/10.1088/1748-9326/ac6888>
- Shah, J., Kumar, R., Samaniego, L., Markonis, Y., Hanel, M., Attinger, S., et al. (2023). On the role of antecedent meteorological conditions on flash drought initialization in Europe. *Environmental Research Letters*, 18(6), 064039. <https://doi.org/10.1088/1748-9326/acd8d3>
- Song, X., Lyu, S., & Wen, X. (2020). Limitation of soil moisture on the response of transpiration to vapor pressure deficit in a subtropical coniferous plantation subjected to seasonal drought. *Journal of Hydrology*, 591, 125301. <https://doi.org/10.1016/j.jhydrol.2020.125301>
- Stanke, C., Kerac, M., Prudhomme, C., Medlock, J., & Murray, V. (2013). Health effects of drought: A systematic review of the evidence. *PLoS Currents*, 5, 1–4. <https://doi.org/10.1371/currents.dis.7a2cee9e980f91ad7697b570bcc4b004>
- Sun, J., & Ao, J. (2013). Changes in precipitation and extreme precipitation in a warming environment in China. *Chinese Science Bulletin*, 58(12), 1395–1401. <https://doi.org/10.1007/s11434-012-5542-z>
- Sundararajan, M., Taly, A., & Yan, Q. (2017). Axiomatic attribution for deep networks. *arXiv:1703.01365[Cs]*. Retrieved from <http://arxiv.org/abs/1703.01365>
- Svoboda, M., LeComte, D., Hayes, M., Heim, R., Gleason, K., Angel, J., et al. (2002). The drought monitor. *Bulletin of the American Meteorological Society*, 83(8), 1181–1190. <https://doi.org/10.1175/1520-0477-83.8.1181>
- Theil, H. (1992). A rank-invariant method of linear and polynomial regression analysis. In B. Raj & J. Koerts (Eds.), *Henri Theil's contributions to economics and econometrics: Econometric theory and methodology* (pp. 345–381). Springer Netherlands. https://doi.org/10.1007/978-94-011-2546-8_20
- Thut, H. F. (1938). Relative humidity variations affecting transpiration. *American Journal of Botany*, 25(8), 589–595. <https://doi.org/10.2307/2436518>
- Toms, B. A., Barnes, E. A., & Ebert-Uphoff, I. (2020). Physically interpretable neural networks for the geosciences: Applications to earth system variability. *Journal of Advances in Modeling Earth Systems*, 12(9), e2020MS002084. <https://doi.org/10.1029/2019MS002002>
- Tyagi, S., Zhang, X., Saraswat, D., Sahany, S., Mishra, S. K., & Niyogi, D. (2022). Flash drought: Review of concept, prediction and the potential for machine learning, deep learning methods. *Earth's Future*, 10(11), e2022EF002723. <https://doi.org/10.1029/2022EF002723>
- Uribe, M. D. R., & Dukes, J. S. (2021). Land cover change alters seasonal photosynthetic activity and transpiration of Amazon forest and Cerrado. *Environmental Research Letters*, 16(5), 054013. <https://doi.org/10.1088/1748-9326/abf60d>
- van Dijk, A. I. J. M., Beck, H. E., Crosbie, R. S., de Jeu, R. A. M., Liu, Y. Y., Podger, G. M., et al. (2013). The Millennium Drought in southeast Australia (2001–2009): Natural and human causes and implications for water resources, ecosystems, economy, and society. *Water Resources Research*, 49(2), 1040–1057. <https://doi.org/10.1002/wrcr.20123>
- Veijalainen, N., Ahopelto, L., Marttunen, M., Jääskeläinen, J., Britschgi, R., Orvoma, M., et al. (2019). Severe drought in Finland: Modeling effects on water resources and assessing climate change impacts. *Sustainability*, 11(8), 2450. <https://doi.org/10.3390/su11082450>
- Wang, L., & Yuan, X. (2018). Two types of flash drought and their connections with seasonal drought. *Advances in Atmospheric Sciences*, 35(12), 1478–1490. <https://doi.org/10.1007/s00376-018-8047-0>
- Wang, L., Yuan, X., Xie, Z., Wu, P., & Li, Y. (2016). Increasing flash droughts over China during the recent global warming hiatus. *Scientific Reports*, 6(1), 30571. <https://doi.org/10.1038/srep30571>
- Wang, M., Menzel, L., Jiang, S., Ren, L., Xu, C.-Y., & Cui, H. (2023). Evaluation of flash drought under the impact of heat wave events in southwestern Germany. *Science of the Total Environment*, 904, 166815. <https://doi.org/10.1016/j.scitotenv.2023.166815>
- Wang, T., Tu, X., Singh, V. P., Chen, X., & Lin, K. (2021). Global data assessment and analysis of drought characteristics based on CMIP6. *Journal of Hydrology*, 596, 126091. <https://doi.org/10.1016/j.jhydrol.2021.126091>
- Wei, Z., Yoshimura, K., Wang, L., Miralles, D. G., Jasechko, S., & Lee, X. (2017). Revisiting the contribution of transpiration to global terrestrial evapotranspiration. *Geophysical Research Letters*, 44(6), 2792–2801. <https://doi.org/10.1002/2016GL072235>
- Wilhite, D. A., Svoboda, M. D., & Hayes, M. J. (2007). Understanding the complex impacts of drought: A key to enhancing drought mitigation and preparedness. *Water Resources Management*, 21(5), 763–774. <https://doi.org/10.1007/s11269-006-9076-5>
- Williams, I. N., & Torn, M. S. (2015). Vegetation controls on surface heat flux partitioning, and land-atmosphere coupling. *Geophysical Research Letters*, 42(21), 9416–9424. <https://doi.org/10.1002/2015GL066305>
- Xi, X., & Yuan, X. (2022). Significant water stress on gross primary productivity during flash droughts with hot conditions. *Agricultural and Forest Meteorology*, 324, 109100. <https://doi.org/10.1016/j.agrformet.2022.109100>
- Xi, X., & Yuan, X. (2023). Remote sensing of atmospheric and soil water stress on ecosystem carbon and water use during flash droughts over eastern China. *Science of the Total Environment*, 868, 161715. <https://doi.org/10.1016/j.scitotenv.2023.161715>
- Yuan, X., Wang, L., Wu, P., Ji, P., Sheffield, J., & Zhang, M. (2019). Anthropogenic shift towards higher risk of flash drought over China. *Nature Communications*, 10(1), 4661. <https://doi.org/10.1038/s41467-019-12692-7>
- Yuan, X., Wang, Y., Ji, P., Wu, P., Sheffield, J., & Otkin, J. A. (2023). A global transition to flash droughts under climate change. *Science*, 380(6641), 187–191. <https://doi.org/10.1126/science.abn6301>
- Zhang, L., Liu, Y., Ren, L., Teuling, A. J., Zhu, Y., Wei, L., et al. (2021). Analysis of flash drought in China using artificial intelligence models. *Hydrology and Earth System Sciences*, 26(12), 3241–3261. <https://doi.org/10.5194/hess-2021-541>
- Zhang, M., Yuan, X., Otkin, J. A., & Ji, P. (2022). Climate warming outweighs vegetation greening in intensifying flash droughts over China. *Environmental Research Letters*, 17(5), 054041. <https://doi.org/10.1088/1748-9326/ac69fb>
- Zhang, Q., Singh, V. P., Sun, P., Chen, X., Zhang, Z., & Li, J. (2011). Precipitation and streamflow changes in China: Changing patterns, causes and implications. *Journal of Hydrology*, 410(3), 204–216. <https://doi.org/10.1016/j.jhydrol.2011.09.017>
- Zhang, Y., You, Q., Mao, G., Chen, C., Li, X., & Yu, J. (2021). Flash drought characteristics by different severities in humid subtropical basins: A case study in the Gan river basin, China. *Journal of Climate*, 34(18), 7337–7357. <https://doi.org/10.1175/JCLI-D-20-0596.1>

- Zhu, B., Xie, X., Meng, S., Lu, C., & Yao, Y. (2020). Sensitivity of soil moisture to precipitation and temperature over China: Present state and future projection. *Science of the Total Environment*, 705, 135774. <https://doi.org/10.1016/j.scitotenv.2019.135774>
- Zhu, Q., & Wang, Y. (2021). The diagnosis about spatiotemporal characteristics and driving factors of flash drought and its prediction over typical humid and semiarid basins in China. *Journal of Hydrometeorology*, 22(10), 2783–2798. <https://doi.org/10.1175/JHM-D-21-0062.1>